Botanical Journal of the Linnean Society, 2024, **XX**, 1–33
https://doi.org/10.1093/botlinnean/boae071
Advance access publication 16 October 2024
Original Article

OXFORD

Original Article
Cuticular morphology of *Schinus* L. and related genera

Theodore P. Matel[1,2,*], Maria A. Gandolfo[2], John D. Mitchell[3]

[1]Department of Earth and Environmental Sciences and Museum of Paleontology, University of Michigan, Ann Arbor, MI, United States
[2]L.H. Bailey Hortorium, Plant Biology Section, School of Integrative Plant Science, Cornell University, Ithaca, NY, United States
[3]The New York Botanical Garden, Bronx, NY, United States

[*]Corresponding author. Department of Earth and Environmental Sciences and Museum of Paleontology, University of Michigan, Ann Arbor, MI, United States.
E-mail: tmatel@umich.edu

ABSTRACT

The Anacardiaceae are a characteristic angiosperm family of the Neotropics where they comprise ~32 genera and 200 species (~80 genera and 800 species globally). Among Neotropical Anacardiaceae genera, *Schinus* has the greatest species richness with 42 species distributed from tropical latitudes of Brazil and Peru south to the temperate steppe, matorral, and Valdivian temperate forest communities of Patagonia. Previous studies have found some anatomical and morphological leaf traits (e.g. simple vs. compound leaf organization) useful in characterizing lineages within *Schinus,* but also document traits that are homoplastic within the genus (e.g. stomatal distribution) and convergent among *Schinus* and its close relatives *Lithrea* and *Mauria* (e.g. mesophyll arrangement). Here, we present a survey of leaf cuticular traits in 53 species of *Schinus* and its closest relatives *Lithrea*, *Mauria*, and *Euroschinus* based on characters observed with scanning electron and optical light microscopy. We use ordinated Bray–Curtis distances based on 18 characters and 2D nonmetric multidimensional scaling to show that cuticular morphology resolves the three most diverse genera, *Euroschinus*, *Mauria*, and *Schinus,* but does not resolve intrageneric sections of *Schinus*. We propose that a distinctive acuminate gland type occurring only within *Euroschinus* may constitute a potential synapomorphy for this genus. Within *Schinus*, we find inconsistency in stomatal distribution among specimens of a single species, among species of a single section, and between sections of the genus, and suggest that current evidence is insufficient to implicate either phenotypic plasticity or homoplasy as the causative mechanism of this variation.

Keywords: Anacardiaceae; amphistomous; cuticle; *Euroschinus*; *Schinus*; stomata

INTRODUCTION

The epidermal surface of angiosperm leaves is a morphologically diverse and multifunctional interface between a leaf and its local environment of light, atmosphere, and biota. Key features of this interface highlighted in ecological, systematic, and palaeobotanical studies include the morphology, size, distribution, and arrangement of stomata (Stace 1965, Woodward 1987, Baranova 1992, Carpenter 2005), and the distribution, morphology, and chemistry of trichomes and glands (Johnson 1975, Carpenter 2006, Lacchia *et al.* 2016). Other features that have not received as much attention but are readily visible under microscopy include the size and shape of epidermal cells and ornamentation of the outer surface of epidermal cell periclinal walls (Dilcher 1974, Wilkinson 1979). Cuticular traits can be used to inform hypotheses about taxon relationships (Upchurch 1984), leaf functionality (Raven 2002), plant–insect interactions (Muller 2006), and palaeoclimate (Royer 2001), and their wide applicability merits investigation of basic cuticular morphology across angiosperms and within focal clades. The objective of this study is to document the cuticular characters present in Anacardiaceae (the cashew family) genera *Schinus* L., *Euroschinus* Hook.f., *Lithrea* Miers ex Hook. & Arn., and *Mauria* Kunth, using scanning electron (SEM) and light microscopy (LM). These four genera, along with the monotypic Australian genus *Rhodosphaera* Haeckel, have been previously resolved as a monophyletic group within a large clade that includes most members of the formerly recognized tribes Anacardiaeae, Dobineae, and Rhoeae (Mitchell and Mori 1987, Pell 2004, Weeks *et al.* 2014, Joyce *et al.* 2023).

Schinus comprises ~42 species placed into eight sections based on the results of molecular phylogenetic analysis (Silva-Luz *et al.* 2019, 2022). These sections are supported by characters and character states such as leaf organization, presence or absence of thorny branches, secondary vein patterns, petal/stamen size ratio, presence of laterally compressed fruits, petiole vasculature, and stomatal distribution (Silva-Luz *et al.* 2019). The sections occur in a variety of ecoregions, including dry and

Received 26 June 2024; revised 6 September 2024; accepted 9 September 2024

Table 1. Herbarium voucher information for the taxa sampled in this study using scanning electron microscopy (SEM) and light microscopy (LM).

Taxon	Herbarium ID	SEM (no. of samples)	LM (no. of samples)
Euroschinus falcatus Hook.fil.	BH294761	1	
Euroschinus falcatus Hook.fil.	BH294762	1	
Euroschinus falcatus Hook.fil.	AQ607689 (NY)	1	2
Euroschinus viellardii Engl.	BH294763	2	
Euroschinus viellardii Engl.	NY	1	1
Euroschinus elegans Engl.	NY	2	1
Euroschinus obtusifolius Engl.	NY	2	1
Euroschinus papuana Merr. & L.M.Perry	NY	2	1
Euroshinus rubromarginata Baker fil.	NY3919025	2	2
Euroschinus verrucosus Engl.	NY	2	1
Lithraea brasiliensis Marchand	BH294785	1	
Lithraea brasiliensis Marchand	BH294784	1	
Lithraea brasiliensis Marchand	NY4165905	1	1
Lithraea caustica Hook & Arn.	BH294786	1	
Lithraea caustica Hook & Arn.	BH294787	1	
Lithraea caustica Hook & Arn.	NY	1	1
Lithraea molleoides (Vell.) Engl.	BH295795	1	
Lithraea molleoides (Vell.) Engl.	BH281149	1	
Lithraea molleoides (Vell.) Engl.	NY1039142	1	1
Mauria cuatrecasasii F.A.Barkley	NY	2	1
Mauria denticulata J.F.Macbr.	NY	2	1
Mauria ferruginea Tul.	NY	1	
Mauria ferruginea Tul.	NY	1	
Mauria heterophylla Kunth.	NY	1	
Mauria heterophylla Kunth.	NY	1	
Mauria heterophylla Kunth.	NY	2	
Mauria heterophylla Kunth.	BH294801	1	
Mauria heterophylla Kunth.	BH294799	1	
Mauria heterophylla Kunth.	NY	1	
Mauria heterophylla Kunth.	BH294797	1	
Mauria heterophylla Kunth.	BH294799	1	
Mauria heterophylla Kunth.	NY		1
Mauria heterophylla Kunth.	NY	1	
Mauria heterophylla Kunth.	NY	1	
Mauria heterophylla Kunth.	NY	1	0
Mauria heterophylla Kunth.	NY	1	0
Mauria peruviana Cuatrec.	NY	1	1
Mauria peruviana Cuatrec.	NY	1	
Mauria sericea Loes.	NY	1	2
Mauria simplicifolia Kunth.	NY	1	1
Mauria simplicifolia Kunth.	NY	1	
Mauria simplicifolia Kunth.	NY	2	
Mauria subserrata Loes.	NY	1	1
Mauria subserrata Loes.	NY	1	
Mauria thaumatophylla Loes.	NY	1	1
Mauria thaumatophylla Loes.	NY3527933	1	
Schinus areira L.	NY2555978	1	1
Schinus areia L.	NY2555982	1	1
Schinus bumelioides I.M.Johnst.	NY	1	1
Schinus bumelioides I.M.Johnst.	NY		1

Table 1. Continued

Taxon	Herbarium ID	SEM (no. of samples)	LM (no. of samples)
Schinus bumelioides I.M.Johnst.	NY	1	
Schinus congestiflora Silva-Luz & Pirani	NY	1	1
Schinus congestiflora Silva-Luz & Pirani	NY	1	
Schinus engleri F.A.Barkley	BH295239	1	
Schinus engleri F.A.Barkley	BH295238	1	
Schinus engleri F.A.Barkley	NY2702142		3
Schinus engleri var. *uruguayensis* F.A. Barkley.	NY	1	2
Schinus fasciculata (Griseb.) I.M.Johnst.	NY2681143	1	1
Schinus fasciculata (Griseb.) I.M.Johnst.	NY		
Schinus ferox Hassl.	NY	1	1
Schinus ferox Hassl.	NY	1	1
Schinus gracilipes I.M.Johnst.	BH295240	2	
Schinus gracilipes I.M.Johnst.	NY	1	2
Schinus johnstonii F.A.Barkley	NY	2	1
Schinus johnstonii F.A.Barkley	NY	1	1
Schinus johnstonii F.A.Barkley	NY	2	
Schinus latifolia (Gillies ex Lindl.) Engl.	BH281540	1	
Schinus latifolia (Gillies ex Lindl.) Engl.	BH281543	2	
Schinus latifolia (Gillies ex Lindl.) Engl.	NY	1	1
Schinus latifolia (Gillies ex Lindl.) Engl.	NY	1	1
Schinus lentiscifolia Marchand	BH295242	2	
Schinus lentiscifolia Marchand	BH281547	1	
Schinus lentiscifolia Marchand	NY	2	1
Schinus longifolia (Lindl.) Speg.	BH281548	1	
Schinus longifolia (Lindl.) Speg.	BH281550	1	
Schinus longifolia (Lindl.) Speg.	NY	1	2
Schinus marchandii F.A.Barkley	NY	1	1
Schinus marchandii F.A.Barkley	NY	1	1
Schinus meyeri F.A.Barkley	NY	1	
Schinus meyeri F.A.Barkley	NY		1
Schinus microphylla I.M.Johnst.	NY	1	
Schinus microphylla I.M.Johnst.	NY	1	1
Schinus minutiflora Silva-Luz & Pirani	NY	1	1
Schinus minutiflora Silva-Luz & Pirani	NY	1	
Schinus molle L.	BH281469	1	
Schinus molle L.	BH281502	1	
Schinus molle L.	NYBG2423641	1	1
Schinus montana (Phil.) Engl.	BH281567	2	
Schinus montana (Phil.) Engl.	NY	1	1
Schinus montana (Phil.) Engl.	NY	1	1
Schinus myrtifolia (Griseb.) Cabrera	BH295243	2	
Schinus myrtifolia (Griseb.) Cabrera	NY	1	1
Schinus myrtifolia (Griseb.) Cabrera	NY		1
Schinus odonellii F.A.Barkley	NY	1	1
Schinus odonellii F.A.Barkley	NY	1	1
Schinus patagonica (Phil.) I.M.Johnst. ex Cabrera	NY	1	1
Schinus patagonica (Phil.) I.M.Johnst. ex Cabrera	NY	1	1
Schinus pearcei Engl.	NY	1	
Schinus pearcei Engl.	NY	1	1
Schinus pilifera I.M.Johnst.	BH295245	2	
Schinus pilifera var. *boliviensis*	NY2681188	1	1

Table 1. Continued

Taxon	Herbarium ID	SEM (no. of samples)	LM (no. of samples)
Schinus pilifera var. *cabrerae*	NY2705618	1	1
Schinus polygama (Cav.) Cabrera	BH295235	1	
Schinus polygama var. *parviflora*	NY2624492	1	
Schinus polygama (Cav.) Cabrera	NY	1	1
Schinus praecox (Griseb.) Speg.	NY	1	1
Schinus praecox (Griseb.) Speg.	NY	1	1
Schinus ramboi F.A.Barkley	NY438031	2	2
Schinus roigii Ruiz Leal & Cabrera	BH121075	2	
Schinus roigii Ruiz Leal & Cabrera	BH121018	2	
Schinus roigii Ruiz Leal & Cabrera	179SA (NYBG)	1	1
Schinus sinuata (Griseb.) Engl.	NY	2	1
Schinus spinosa Engl.	NY2423637	1	
Schinus spinosa Engl.	NY438028	1	1
Schinus terebinthifolia Raddi	BH129228	1	
Schinus terebinthifolia Raddi	BH295517	2	
Schinus terebinthifolia Raddi	NY632025	2	1
Schinus venturii F.A.Barkley	NY	1	1
Schinus venturii F.A.Barkley	NY	1	
Schinus velutina (Turcz.) I.M.Johnst.	NY	1	1
Schinus velutina (Turcz.) I.M.Johnst.	NY	1	1
Schinus weinmannifolia Engl.	BH281552	2	
Schinus weinmannifolia Engl.	NY	1	1
Schinus weinmannifolia Engl.	NY	1	

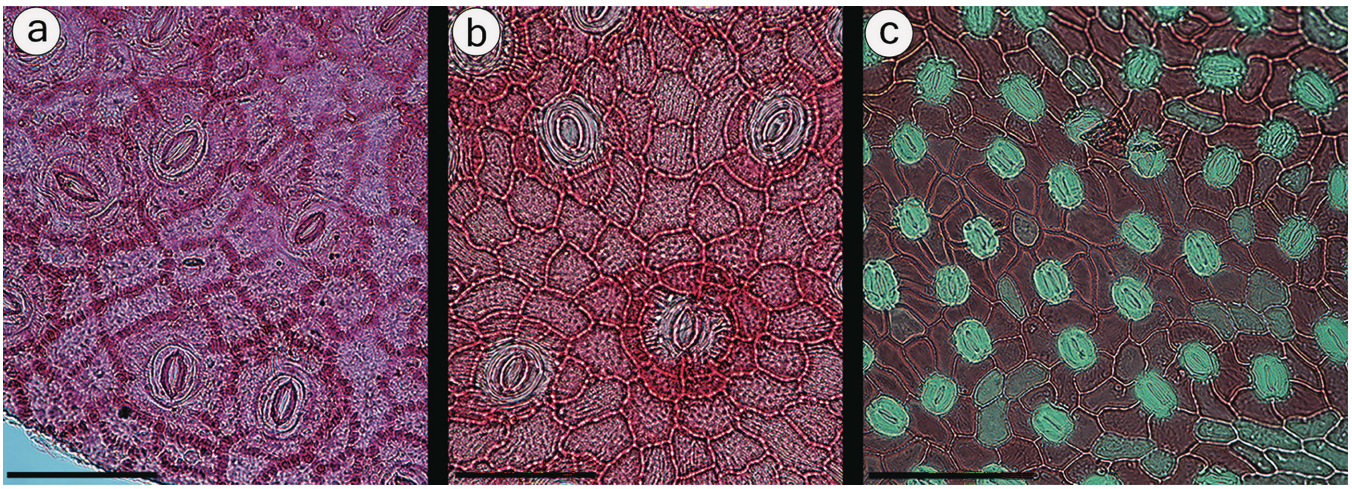

Figure 1. Types of stomatal complexes. A, abaxial surface of *Schinus patagonica* showing anomocytic arrangements of 5–7 contact cells. B, abaxial surface of *Schinus myrtifolia* showing cyclocytic stomatal complexes with 5–7 subsidiary cells; note concentric rings of cells encircling the guard cell pair in the centre of the image. C, abaxial surface of *Mauria thaumatophylla* showing anomocytic stomatal complexes with 4–6 subsidiary cells; subsidiary cells frequently abut more than one guard cell. All scale bars = 100 μm.

moist, Andean and lowland environments from tropical latitudes in Brazil and Peru south to Patagonia (Pell *et al.* 2011; Silva-Luz *et al.* 2019, 2022). *Mauria* comprises 10–15 species occurring in tropical montane and dry forests from El Salvador south to eastern Venezuela and extreme northern Argentina (Pell *et al.* 2011; Mitchell *et al.* 2022); however, it is in need of taxonomic revision. *Lithrea* (also sometimes written as *Lithraea*) includes three species. *Lithrea brasiliensis* Marchand occurs in coastal areas in Brazil; *L. molleoides* (Vell.) Engl. occurs in coastal and lowland subtropical forests of eastern Brazil, Argentina, and Bolivia; while *L. caustica* Hook. & Arn. is found in the Chilean matorral. *Euroschinus* comprises nine or more species, seven in New Caledonia, *E. falcata* Hook.fil. distributed in eastern Australian rainforests and dry forests, and *E. papuana* Merr &

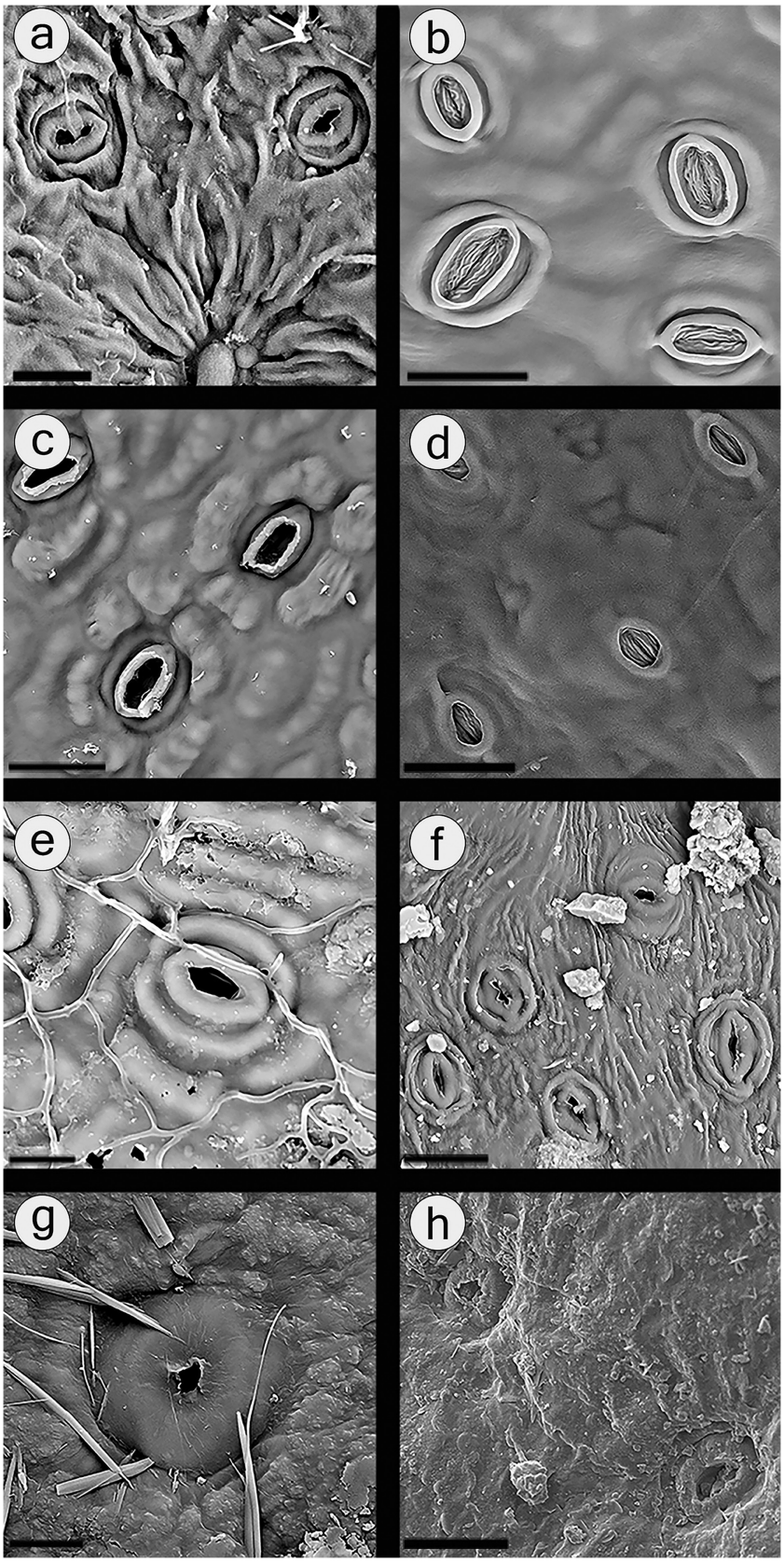

Figure 2. Types of stomatal complex surface morphology. A, Type I complex: abaxial surface of *Euroschinus falcata* showing stomatal complexes with outer stomatal ledges and a peristomal rim below the level of the cuticular surface. Scale bar = 30 μm. B, Type II complex: abaxial surface of *Mauria heterophylla* showing stomatal complexes with slightly sunken outer stomatal ledges and a peristomatal rim level with the cuticular surface; note the cutin frill which adorns the interior of the antechamber. Scale bar = 30 μm. C, Type III complex: abaxial surface of *Lithrea caustica* showing stomatal complexes with slightly sunken outer stomatal ledges and a peristomatal rim that may be sunken or absent;

Table 2. Classification scheme for stomatal complex surface morphology; see Figure 2 for illustrations of representative types.

Stomatal complex type	Peristomal rim		Peristomatal rim position		Outer stomatal ledge position		Outer stomatal ledge shape	
	Present	Absent	Level	Sunken	Level	Sunken	Flat	Domed
Type I	X			X		X		X
Type II	X		X			X		X
Type III		X				X		X
Type IV		X			X			X
Type V	X		X		X			X
Type VI		X			X		X	
Type VII		X				X	X	

L.M. Perry in New Guinean rainforests (Hoff 1994, Morat *et al.* 2012).

The most comprehensive study of cuticular characters in the Anacardiaceae is an unpublished PhD thesis that includes 200 species in 46 genera with 1–16 specimens examined per species (Wilkinson 1971). Subsequent Anacardiaceae cuticle studies are few and have targeted a genus (*Gluta* L.; Wilkinson 1983), species groups (*Rhus* subgenus *Rhus*; Hardin and Phillips 1985), or populations (*Pistacia atlantica* Desf.; Belhadj *et al.* 2007). Some studies have used cuticular characters to identify fossil species of *Pseudosmodingium* Engl. (Ramirez *et al.*, 2000), *Gluta* (Prasad *et al.*, 2013), and *Choerospondias* B.L. Burtt & A.W. Hill (Xiao *et al.* 2022). Characters utilized include cuticle thickness, domatia, trichome morphology and structure, epidermal cell periclinal wall ornamentation, stomatal surface morphology, hydathode stomata, and epidermal cell anticlinal wall thickness (Wilkinson 1971). Of these characters, trichomes appear to have the most systematic utility. Multicellular stalked glands have been identified as a synapomorphy for the subfamily Spondiadeae (Terrazas 1994; =Spondiodeae), equivalent to clades S1 and S2 of Weeks *et al.* (2014) or clade A1 in Joyce *et al.* (2023). Stellate trichomes have been distinguished as a synapomorphy for a group of fossil and living species in *Pseudosmodingium* (Ramirez *et al.*, 2000; Aguilar-Ortigoza *et al.*, 2004). In this contribution, we present light and electron micrographs of the cuticle surface of *Schinus* and its closest relatives, *Euroschinus*, *Mauria*, and *Lithrea*. This study augments our knowledge of Anacardiaceae by providing new cuticle morphology data and discussing its variability in a statistical and phylogenetic context.

MATERIALS AND METHODS

Sampling

In total, 132 herbarium specimens representing 53 species and four varieties in the genera *Euroschinus*, *Mauria*, *Lithrea*, and *Schinus* were sampled from the New York Botanical Garden (NY) and L.H. Bailey Hortorium, Cornell University (BH) herbaria. For SEM, leaves from two to three different voucher specimens were studied for each species unless only a single specimen of a species was available, in which case two to three different leaves were sampled from a single specimen (Table 1). SEM samples were prepared by excising two rectangles with an area of ~5 mm^2 from across the midrib of dry leaves, mounting them on stubs to show the adaxial and abaxial sides, and coated with gold using a sputter-coater (Ted Pella). The leaf material was extracted directly from herbarium voucher specimens and not chemically treated prior to observation and imaging using a desktop Phenom XL SEM (Phenom-World B. V., Eindhoven, The Netherlands) at the L.H. Bailey Hortorium, Cornell University, Ithaca, NY, USA. For LM, one to two specimens were prepared from each species by immersing dry leaf tissue into vials containing 35% H_2O_2 and heating them to 60–70°C for a period of 24–48 h. Cuticle was isolated and cleaned with a fine brush, washed in 75% ethanol, dyed in 2% safranin, left to air dry, and mounted in phenol glycerin jelly. Samples were observed and photographed using a Lumenera Infinity X CMOS camera (Lumenera Corp., Ottawa, Ontario, Canada) connected to an Olympus BH2 microscope (Olympus Corp., Shinjuku, Tokyo, Japan) at the L.H. Bailey Hortorium. SEM stubs and microscopy slides are housed at the Cornell University Plant Anatomy collection (CUPAC) under the BH and NYBG herbarium sheet numbers (Table 1).

Terminology

An effort was made to apply terms used in previous investigations of Anacardiaceae epidermal surface (Wilkinson 1971, 1983, Hardin and Phillips 1985) when writing the descriptions. If the existing terminology proved inadequate, general references were consulted for stomata (Dilcher 1974, Wilkinson 1979, Baranova

note the thickened cuticle on subsidiary cell periclinal walls. Scale bar = 30 μm. D, Type IV complex: abaxial surface of *E. papuana* showing stomatal complexes with outer stomatal ledges level with the epidermal surface and lacking a peristomatal rim; note the polar extensions parallel to the long axis of the stoma. Scale bar = 30 μm. E, Type V complex: abaxial surface of *L. brasiliensis* showing a stomatal complex with outer stomatal ledges and a peristomatal rim level with the epidermal surface. Scale bar = 10 μm. F, Type V complex: abaxial surface of *Schinus lentiscifolia* showing stomatal complexes with outer stomatal ledges and peristomatal rims level with the cuticular surface; note striated peristomatal rims in some complexes. Scale bar = 30 μm. G, Type VI complex: abaxial surface of *S. weinmannifolia* showing a stomatal complex with flat outer stomatal ledges level with the cuticular surface and missing a peristomatal rim. Scale bar = 10 μm. H, Type VII complex: abaxial surface of *S. marchandii* showing stomatal complexes with flat outer stomatal ledges sunken relative to the cuticular surface and lacking a peristomatal rim. Scale bar = 30 μm.

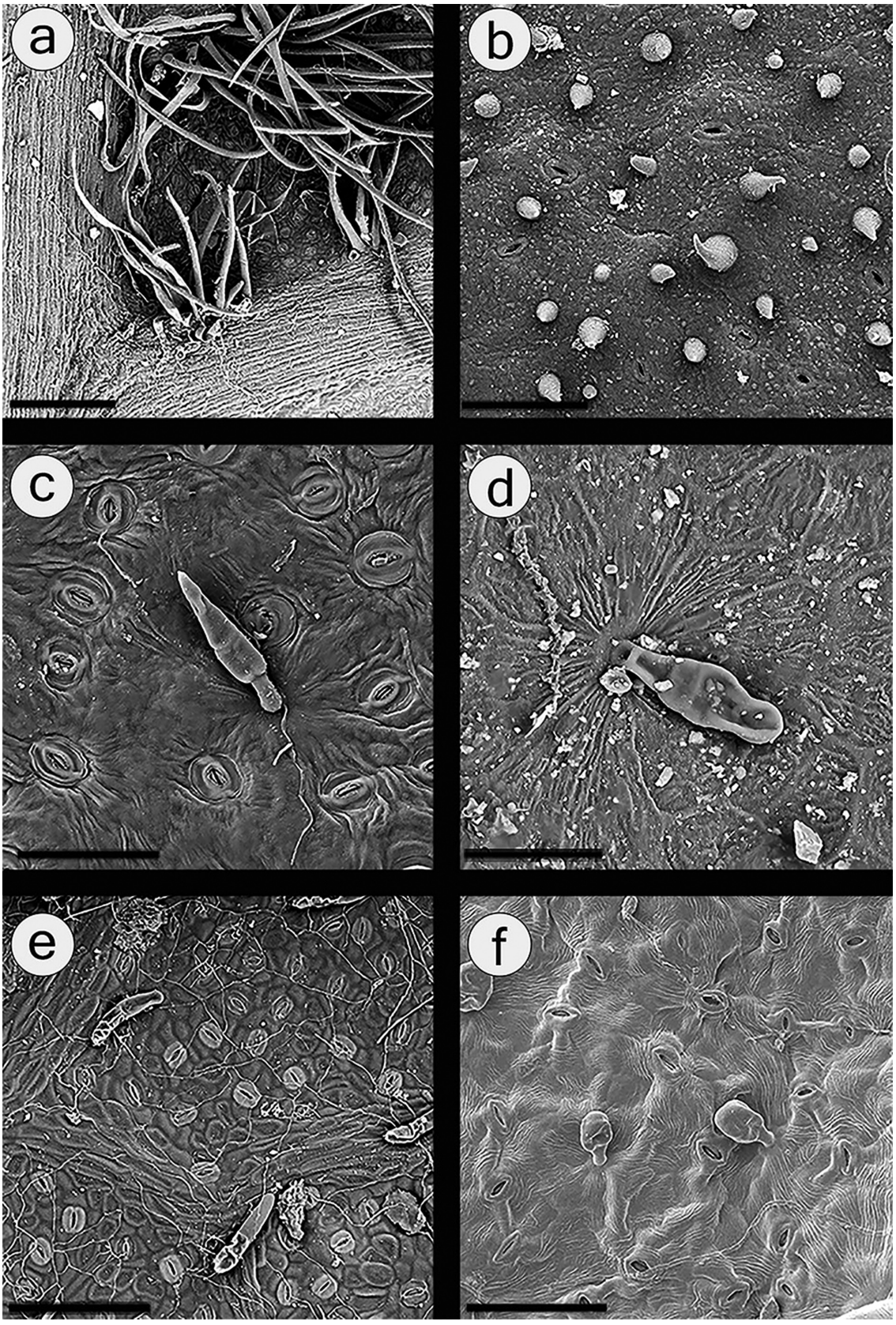

Figure 3. Types of trichomes. A, abaxial surface of *M. thaumatophylla* showing a secondary vein axil with a hair-tuft domatium composed of acicular and ribbon-like simple trichomes. Scale bar = 200 μm. B, abaxial surface of *S. johnstonii* showing conical simple trichomes. Scale bar = 100 μm. C, abaxial surface of *E. obtusifolia* showing an acuminate cylindrical gland. Scale bar = 50 μm. D, adaxial surface of *S. lentiscifolia* showing a short-stalked cylindrical gland. Scale bar = 50 μm. E, abaxial surface of *M. denticulata* showing long-stalked cylindrical glands. Scale bar = 100 μm. F, abaxial surface of *S. pilifera* var. *cabrera* showing bulbous glands. Scale bar = 80 μm.

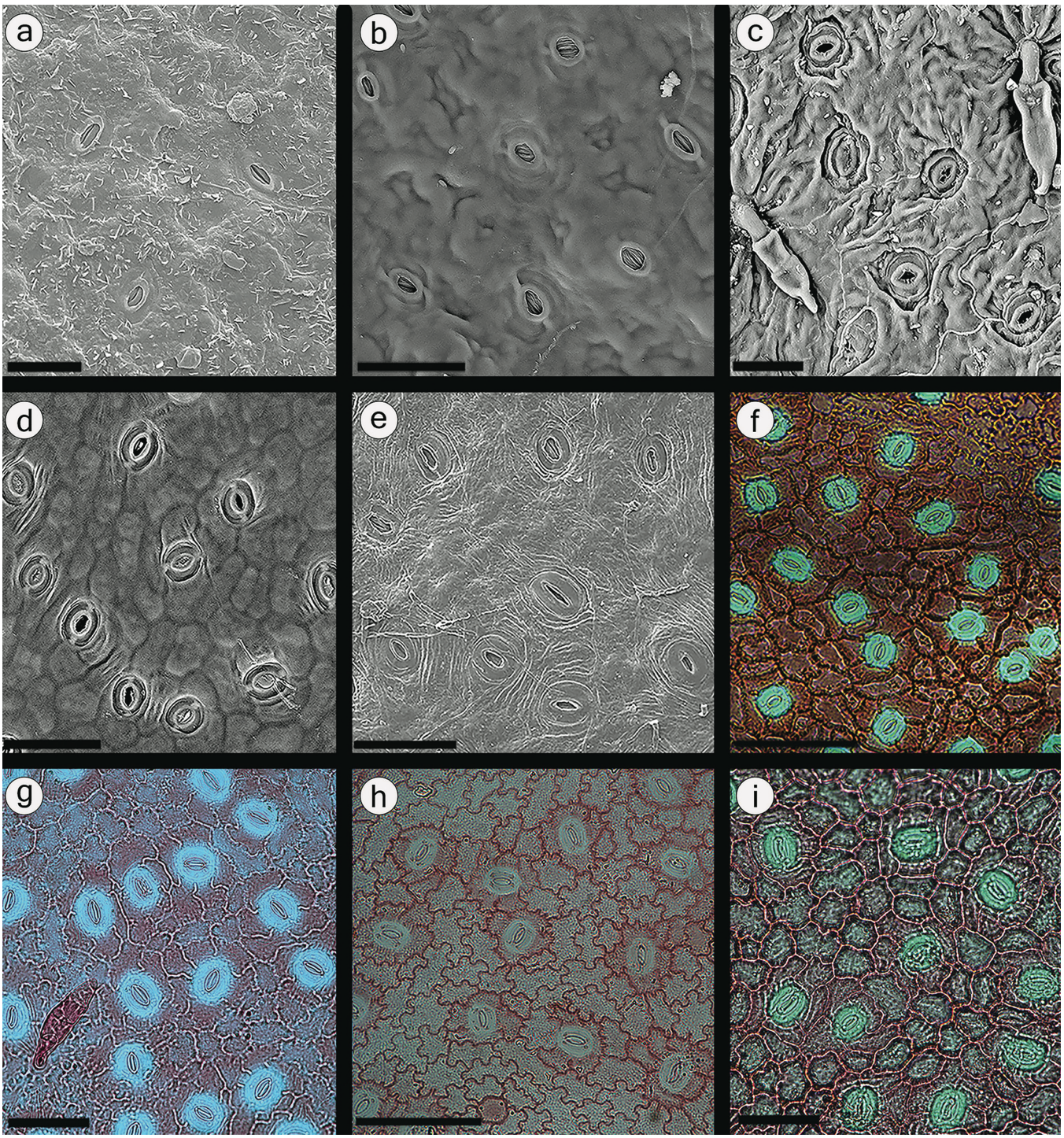

Figure 4. Stomatal complexes of *Euroschinus*. A, abaxial surface of *E. viellardii* showing stomatal complexes with protruding outer stomatal ledges and lacking a peristomatal rim; note angular wax flakes which ornament the surface. Scale bar = 20 μm. B, abaxial surface of *E. papuana* showing stomatal complexes with well-developed outer stomatal ledges and lacking a peristomatal rim; note striations of the interior antechamber and polar extensions of the outer stomatal ledges. Scale bar = 30 μm. C, abaxial surface of *E. falcata* showing stomatal complexes with sunken outer stomatal ledges and peristomatal rims, and acuminate cylindrical glands. Scale bar = 30 μm. D, abaxial surface of *E. verrucosus* showing stomatal complexes with protruding outer stomatal ledges which are slightly sunken, and a peristomatal rim level with the epidermal surface. Scale bar = 30 μm. E, abaxial surface of *E. obtusifolia* showing stomatal complexes with minute, protruding outer stomatal ledges and a peristomatal rim absent or formed by circumstomatal striae. Scale bar = 50 μm. F, abaxial surface of *E. rubromarginata* showing anomocytic stomatal complexes with 4–5 contact cells. Scale bar = 100 μm. G, abaxial surface of *E. obtusifolia* showing anomocytic stomatal complexes with 5–6 contact cells and an acuminate cylindrical gland. Scale bar = 100 μm. H, abaxial surface of *E. viellardii* showing cyclocytic stomatal complexes with subsidiary cells with poorly preserved anticlinal walls; cell walls of neighbouring unspecialized epidermal cells are highly sinuous. Scale bar = 100 μm. I, abaxial surface of *E. elegans* showing cyclocytic stomatal complexes with 4–6 subsidiary cells. Scale bar = 100 μm.

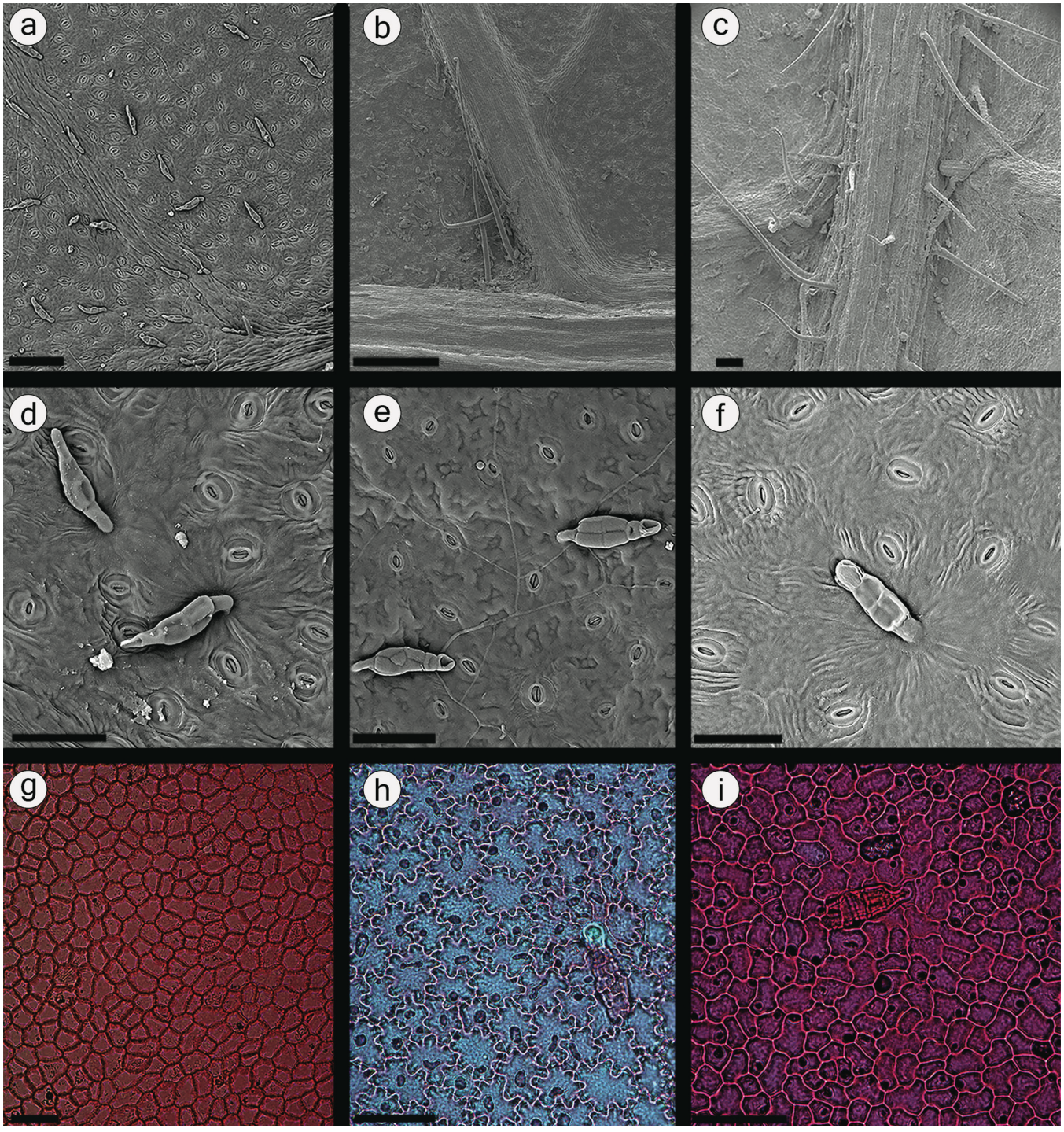

Figure 5. Trichome types and distribution, and epidermal cell shape in *Euroschinus*. A, abaxial surface of *E. obtusifolia* showing a cluster of acuminate cylindrical glands in the axil of a primary vein. Scale bar = 100 μm. B, abaxial surface of *E. falcata* showing a weakly developed hairy-tuft domatium in the axil of a primary vein. Scale bar = 100 μm. C, abaxial surface of *E. viellardii* showing pilose-glandular trichome cover along the midrib. Scale bar = 100 μm. D, abaxial surface of *E. obtusifolia* showing cylindrical acuminate glands with one or two multicellular tiers and two apical unicellular tiers. Scale bar = 50 μm. E, abaxial surface of *E. papuana* showing conical acuminate glands with a body composed of two multicellular tiers and two unicellular tiers. Scale bar 50 μm. F, abaxial surface of *E. elegans* showing a cylindrical gland with a singular, rounded apical cell. Scale bar = 50 μm. G, adaxial surface of *E. verrucosus* showing epidermal cells with straight or rounded anticlinal walls. Scale bar = 100 μm. H, abaxial surface of *E. elegans* showing epidermal cells with sinuous anticlinal walls and a gland base surrounded by six unspecialized epidermal cells. Scale bar = 100 μm. I, adaxial surface of *E. papuana* showing epidermal cells with wavy anticlinal walls and a gland base surrounded by six epidermal cells. Scale bar = 100 μm.

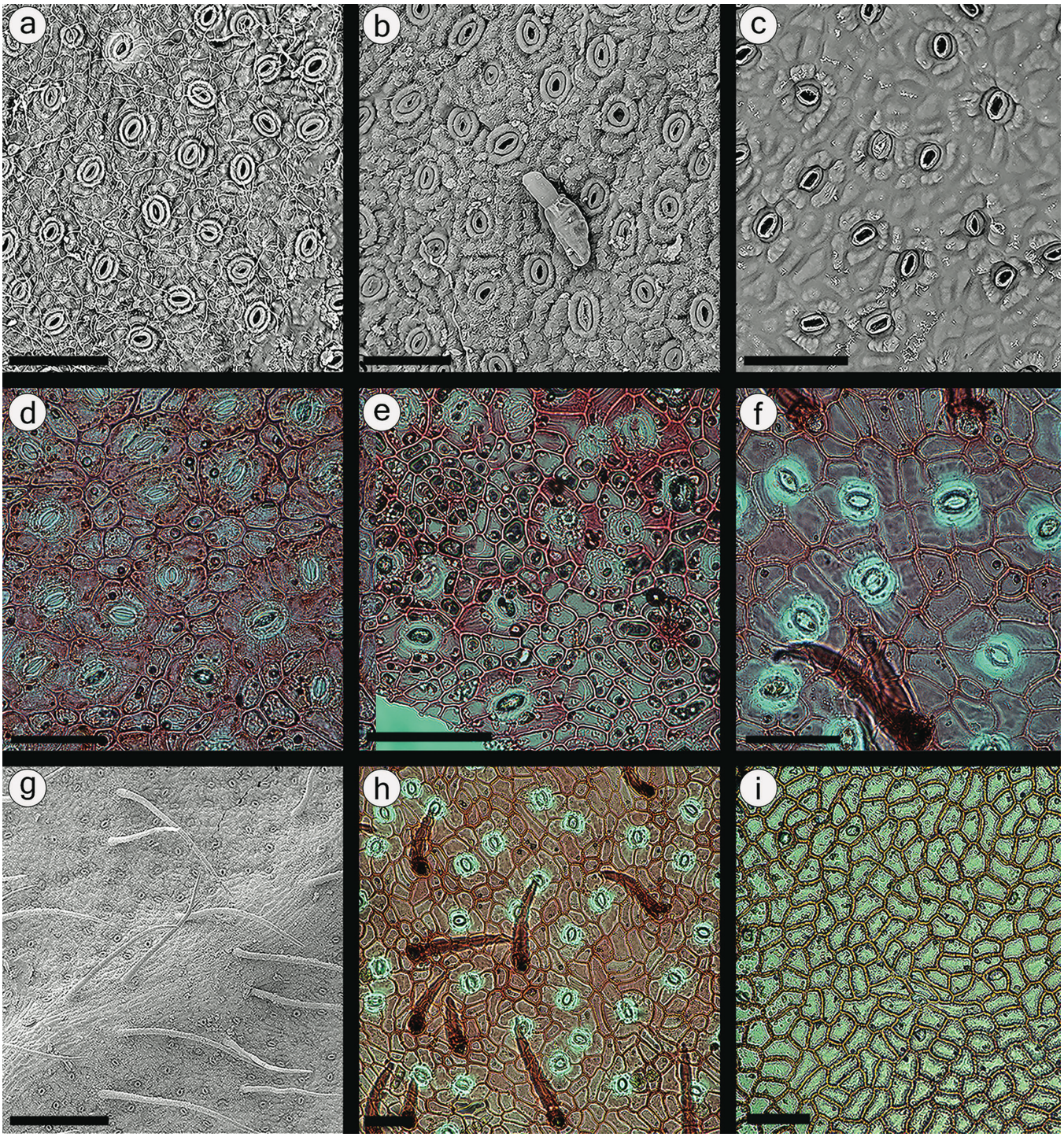

Figure 6. Cuticular features in *Lithrea*. A, SEM micrograph of the abaxial surface of *L. brasiliensis* showing stomatal complex surface morphology; note consecutive rings encircling the stoma formed by outer stomatal ledges, the peristomatal rim, and cuticular thickenings on subsidiary cell periclinal walls. Scale bar = 80 μm. B, abaxial surface of *L. molleoides* showing a cylindrical-uniseriate gland, stomatal complexes, and wax flakes. Scale bar = 100 μm. C, abaxial surface of *L. caustica* showing sunken, cup-shaped stomatal ledges and cyclocytic subsidiary cells with thickened periclinal walls. Scale bar = 50 μm, D, light micrograph of the abaxial surface of *L. brasiliensis* showing epidermal cells and stomatal complexes; note the radially elongated subsidiary cells of the stomatal complex 1. Scale bar = 100 μm. E, abaxial surface of *L. molleoides* showing epidermal cells and cycloyctic subsidiary cells 2. Scale bar = 100 μm. F, abaxial surface of *L. caustica* showing anomocytic 3 and staurocytic 4 stomatal complexes. Scale bar = 100 μm. G, abaxial surface of *L. caustica* showing simple acicular trichomes clustered near a secondary vein. Scale bar = 300 μm. H, abaxial surface of *L. caustica* showing epidermal cells, stomatal complexes, and simple acicular trichomes and trichomes bases. Scale bar = 100 μm. I, adaxial surface of *L. caustica* showing epidermal cells with straight or slightly curved epidermal cells. Scale bar = 100 μm.

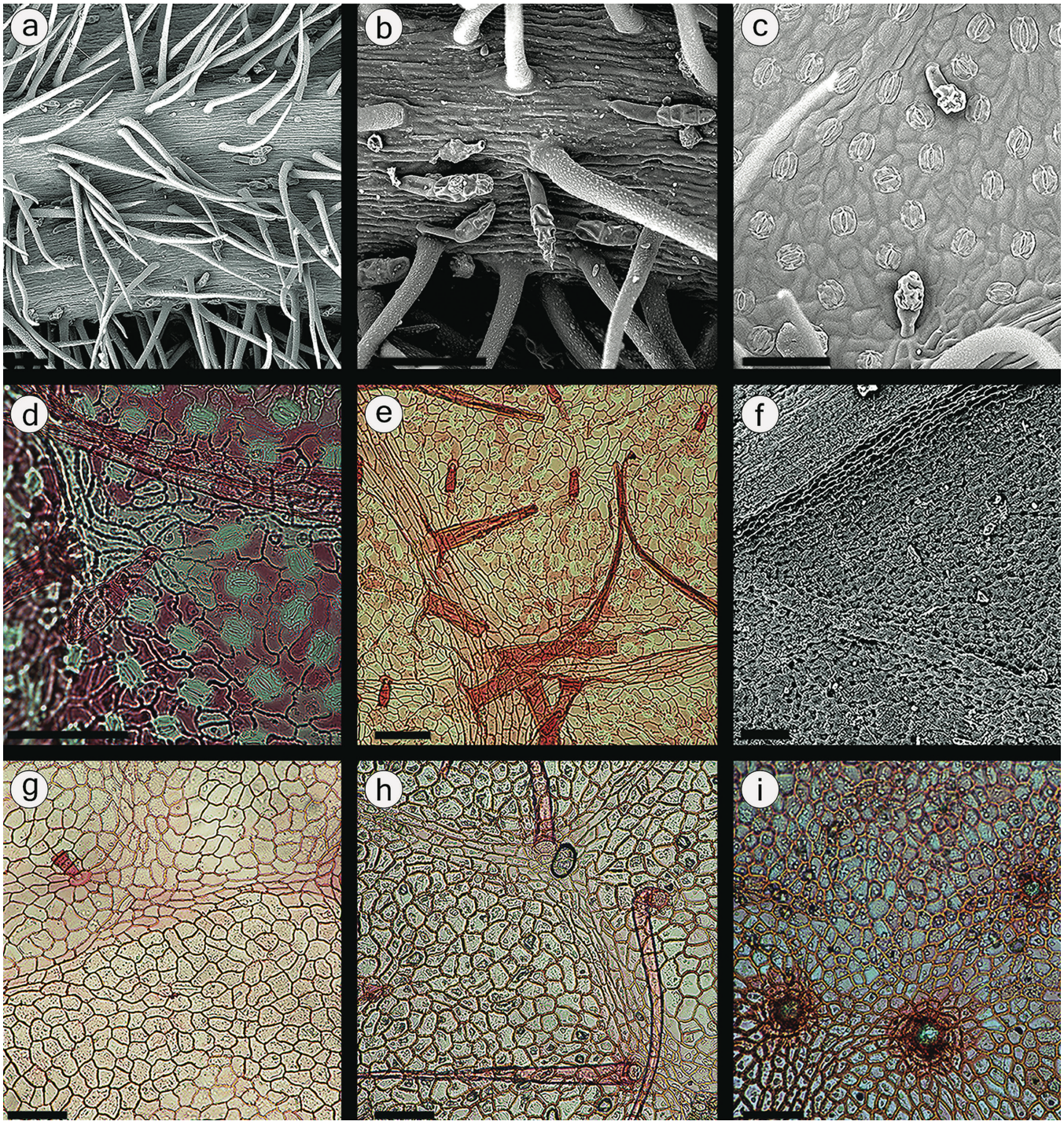

Figure 7. Trichome types and epidermal cells in *Mauria*. All scale bars = 100 μm. A, SEM micrograph of *M. ferruginea* showing pilose-glandular pubescence on the abaxial midvein. B, close-up of long-stalked cylindrical glands on the abaxial midvein of *M. feruginea*; gland bodies are uniseriate with three or four tiers. C, abaxial surface of *M. subserrata* showing glands with multiseriate ovoid heads and a short, unicellular stalk. D, light micrograph of *M. subserrata* showing a uniseriate, cylindrical gland surrounded at the base by radially elongated epidermal cells. E, abaxial surface of *M. cuatrecasasii* showing ribbon-like simple trichomes and long-stalked cylindrical glands; note the lightly staining bodies of glands in contrast with the darkly staining bodies. F, glabrous adaxial surface of *M. heterophylla*. G, adaxial surface of *M. cuatrecasasii* showing epidermal cells with curved walls and the base of a gland surrounded by nine cyclically arranged epidermal cells. H, adaxial surface of *M. subserrata* showing epidermal cells with straight anticlinal walls and acicular trichomes. I, adaxial surface of *M. ferruginea* showing trichome bases surrounded by multiple rings of cyclocytically arranged and darkly staining epidermal cells.

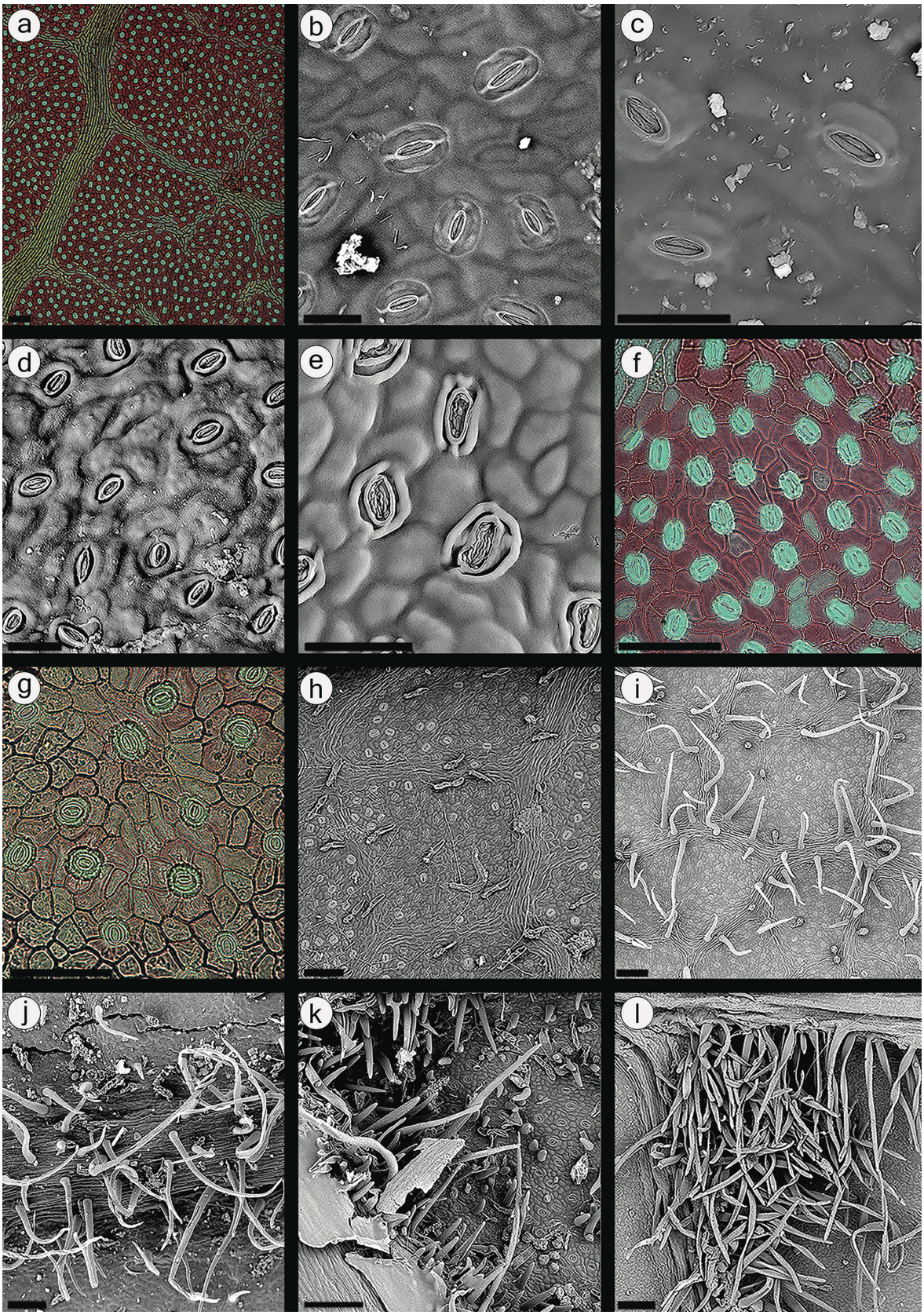

Figure 8. Stomatal complexes and vestiture in *Mauria*. A, light micrograph of the abaxial surface of *M. thaumatophylla* showing densely distributed stomata and a freely ending veinlet. Scale bar = 100 μm. B, SEM micrograph of the abaxial surface of *M. ferruginea* showing stomatal complexes with thin, protruding outer stomatal ledges, a faint peristomatal rim, and cylcocytic subsidiary cells with cuticular thickenings on the periclinal wall. Scale bar = 20 μm. C, abaxial surface of *M. cuatrecasasii* showing stomatal complexes with a narrow, oval aperture and interior antechamber ornamented with fine striae. Scale bar = 20 μm. D, abaxial surface of *M. heterophylla* showing stomatal complexes with

1987, 1992), and trichome types and indumentum (Uphof 1963, Payne 1978, Theobald *et al.* 1979). The scope and format of descriptions follow Stace (1965).

Stomatal distribution

Three patterns of stomatal distribution are commonly recognized within angiosperms according to which leaf surfaces possess stomata. Hypostomous leaves have stomata only on the abaxial (lower) surface, and this is the predominant condition among angiosperms (Muir 2015). Epistomous leaves possess stomata on the adaxial (upper) surface, and amphistomous leaves have numerous and widely distributed stomata on lower and upper leaf surfaces. Previous authors (Wilkinson 1971, Silva-Luz *et al.* 2019) have recognized a pattern in Anacardiaceae in which stomata are widely distributed on the abaxial surface but restricted to a few bands along the midvein and secondary vein axils on the adaxial surface. Pole (2010) observed this pattern in Australasian members of the Sapindaceae and labelled the condition partially amphistomous. We apply the term partially amphistomous only to describe species with apparent spatial restriction of stomata on the adaxial surface.

Stomatal complex types

Our classification of stomatal complexes follows the definitions from Dilcher (1974) and Baranova (1987), combined with images and drawings from Dilcher (1974), Baranova (1987, 1992), and Yaojia *et al.* (1999), as repurposed by Barclay *et al.* (2007). We consider the stomatal complex to encompass a pair of guard cells and all adjacent cells that contact their anticlinal walls. Subsidiary cell is applied only to contact cells that differ from ordinary epidermal cells. Wilkinson (1971) surveyed ~200 species of 46 Anacardiaceae genera and concluded that in nearly all the species, stomata have 4–8 contact cells and their configurations include actinocytic, anomocytic (Fig. 1A), and cyclocytic (Fig. 1B) types. Cyclocytic (Fig. 1B) complexes have a single ring of five or more small cells that encloses the guard cells and anticlinal walls of subsidiary cells are tangential to guard cells. In anomocytic complexes (Fig. 1A, C), guard cells are adjacent to five or more contact cells, and contact cells are not differentiated in any way from normal epidermal cells. The only other type of stomatal complex that occurs within the Anacardiaceae is the paracytic type, known to be found in *Dracontomelon* Blume, *Anacardium occidentale* L., *Pseudospondias macrocarpa* (A. Rich.) Engl., and some species of *Spondias* L. (Wilkinson 1971).

Stomatal surface morphology

Cuticle ornamentation on the periclinal walls of the cells comprising the stomatal complex forms distinctive micromorphological patterns (Stace, 1965b, Wilkinson 1979). Wilkinson (1971: fig. iii, A–F) recognized six distinct patterns of cuticle ornamentation around stomatal complexes by studying leaves in cross-section. The outer stomatal ledges and the peristomatal rim, two characters important to this classification scheme, are visible in SEM surface view and appear to be consistent within species. Outer stomatal ledges are cuticular projections that arise from the periclinal surface of guard cells and may form a dome-shaped vestibule (antechamber) over the stomatal pore (Fig. 2A–F) or be flattened (Fig. 2G, H). The peristomatal rim is formed by cuticular ridges developing along the shared periclinal wall of guard cells and subsidiary cells (Fig. 2A, B, E, F). Additional characters that may distinguish stomatal complexes in surface view are polar cutin rods which extend parallel to the long axis of the stoma from the outer stomatal ledge (Fig. 2D), striations of the peristomatal rim or interior of the antechamber (Fig. 2B), and cuticular thickenings on the periclinal surface of subsidiary cells (Fig. 2C). We distinguish seven types of stomatal surface morphology based on the position of the base of outer stomatal ledges relative to the pavement cell zone, the position of the apex of outer stomatal ledges relative to the pavement cell zone, the presence or absence of a peristomatal rim, and the position of the peristomatal rim relative to the outer stomatal ledges (Fig. 2; Table 2; Supporting Information, Appendix S1).

Trichome types

Anacardiaceae have simple, stalked, and stellate trichomes, which may be glandular or not, and peltate scales (Wilkinson 1971, Pell *et al.* 2011; Mitchell *et al.* 2022). Simple trichomes include unicellular and uniseriate-multicellular types, and these two are often difficult to distinguish owing to the thinness of the septa between cells of the uniseriate-multicellular variety. Simple trichomes occur in three distinct morphologies: acicular or subulate trichomes (Fig. 3A, lower left), filiform or ribbon-like trichomes (Fig. 3A, middle and upper right) that are of similar size to acicular trichomes and appear to intergrade with them in some specimens, and short, conical trichomes (Fig. 3B). The acicular type is very common in the Anacardiaceae, but filiform and conical types have only been observed in a few species—filiform trichomes in *Cotinus coggygria* Scop., and conical trichomes in

sunken stomatal ledges. Scale bar = 30 μm. E, abaxial surface of *M. simplicifolia* showing stomatal complexes with sunken outer stomatal ledges and well-developed cuticular striae in the interior of the antechamber. Scale bar = 20 μm. F, abaxial surface of *M. thaumatophylla* showing cyclocytic and anomocytic subsidiary cell arrangement in stomatal complexes; note adjacent pairs of guard cells which share one or more subsidiary cells. Scale bar = 100 μm. G, abaxial surface of *M. peruviana* showing cyclocytic stomatal complexes and more widely spaced stomata. Scale bar = 100 μm. H, abaxial surface of *M. denticulata* showing a cluster of glands surrounding an areole (glandular vestiture). Scale bar = 100 μm. I, abaxial surface of *M. subserrata* showing a cluster of simple trichomes and glands surrounding an areole (pilose-glandular vestiture). Scale bar = 100 μm. J, adaxial surface of *M. ferruginea* showing a midvein with pilose vestiture of acicular trichomes. Scale bar = 100 μm. K, abaxial surface of *M. heterophylla* showing a tuft-domatium composed of acicular and conical trichomes. Scale bar = 100 μm. L, abaxial surface of *M. heterophylla* showing a primary vein axil with a well-developed tuft-domatium composed of acicular and ribbon-like trichomes. Scale bar = 100 μm.

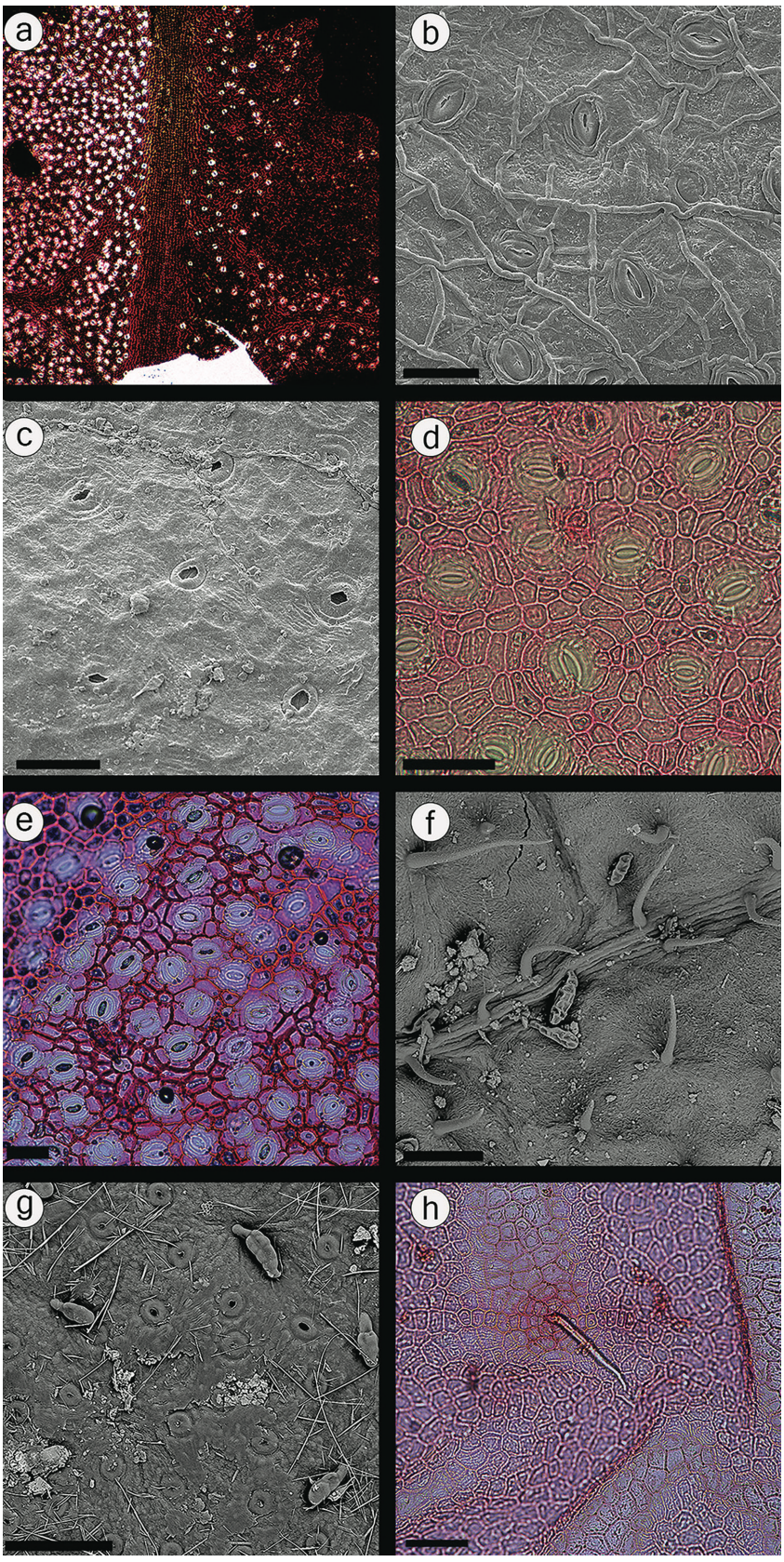

Figure 9. Cuticular features in *Schinus* section *Terebinthifolia*. A, light micrograph of *S. weinmannifolia* showing the distribution of stomata on the abaxial (left) and adaxial (right) surfaces. Scale bar = 100 μm. B, SEM micrograph of the abaxial surface of *S. terebinthifolia* showing stomatal complexes with protruding stomatal ledges and a striate peristomatal rim. Scale bar = 30 μm. C, adaxial surface of *S. weinmannifolia* showing stomatal complexes with flat stomatal ledges. Scale bar = 50 μm. D, abaxial surface of *S. terebinthifolia* showing cyclocytic subsidiary cells and unspecialized epidermal cells with straight or rounded anticlinal walls. Scale bar = 100 μm. E, abaxial surface of *S. weinmannifolia*

two spondioid species *Spondias mombin* Jacq. and *Semecarpus rufo-velutinus* Ridl. (Wilkinson 1971). The bases of simple trichomes are surrounded by one or multiple rings of 4–10 cells. The shape, size, and orientation of these cells are variable; they can resemble unspecialized epidermal cells, or they may be distinctly elongated and rectangular, wedge-shaped and radially oriented, or reduced and isodiametric with thickened anticlinal walls.

Anacardiaceae glandular trichomes are composed of a unicellular or multicellular stalk and unicellular, multicellular uniseriate, or multicellular multiseriate glands (Fig. 3C–F). Glandular trichomes with multicellular stalks only occur in the subfamily Spondioideae (Terrazas 1994). Wilkinson (1971) classified glandular trichomes by their gland shapes into globose (Fig. 3F), ovoid, oblong-ovoid, and cylindrical (Fig. 3C–E) types. In this study, glandular trichomes are divided into four morphological types according to the number and shape of cells comprising the gland and the relative sizes of the gland and stalk. Acuminate-cylindrical glandular trichomes (Fig. 3C) have a short, unicellular stalk, and a cylindrical or conical gland with two or more multicellular layers and one or two unicellular layers which form an acute to acuminate apex. Short-stalked ovoid glandular trichomes (Fig. 3F) have a short, unicellular stalk and globose-ovoid gland with 1–4 unicellular or bicellular tiers, whereas long-stalked cylindrical ones (Fig. 3E) have long, unicellular stalks and cylindrical, multicellular, and thinly cutinized glands. Short-stalked multiseriate cylindrical glandular trichomes (Fig. 3D) have a short, unicellular, or rarely bicellular stalk and a cylindrical gland with 3–5 multicellular tiers.

Indumentum

The leaf indumentum is affected by intraspecific variability in response to leaf phenology and ontogeny, and local environmental conditions (Johnson 1975). The classification of indumentum in this study draws on the glossary of Payne (1978), and four types are recognized based on the distribution and structure (e.g. glandular or simple) of the trichomes. Puberulent indumentum is characterized by trichomes being sparsely distributed, occurring occasionally along the midrib and major veins, and rarely present between veins**.** Pubescent indumentum defines surfaces in which acicular trichomes are conspicuously present, densely distributed along the midrib and major veins, occasionally present between veins, and much more numerous than glandular trichomes. Glandular indumentum is used when glandular trichomes are widely and densely distributed, occurring along the midrib, major veins, and between veins, and simple trichomes are sparse. Glandular-pubescent indumentum is characteristic of leaves in which simple, acicular, and glandular trichomes are widely distributed and their distribution is dense in certain areas. A number of domatia types have been reported in the Anacardiaceae, including marsupiform, lebetiform, cavernose, axillary hair-tuft, and axillary gland-patch types (Wilkinson 1971; Pell *et al.* 2011).

Cuticular ornamentation

The external surface of the periclinal wall of epidermal cells exhibits micromorphological ornamentation of epicuticular waxes that form striae, granules, and platelets varying in their size, orientation, and density (Wilkinson 1971, 1979, Barthlott *et al.* 1998). Cuticular striae occur in thin, continuous bands stretching over the surface of many epidermal cells, and frequently ornament stomatal complexes or peristomatal rims in radial bands or concentric rings. Wax granules and platelets may appear embedded in cuticle and vary in their degree of angularity.

Epidermal cell anticlinal walls

The anticlinal walls of unspecialized (pavement) epidermal cells are straight, rounded, or undulate; when undulate, anticlinal walls vary in shape, amplitude, and period (Dilcher 1974). In some genera (e.g. *Quercus* L., *Platanus* L.) these variations have been shown to have an environmental basis with shade-leaves developing more undulate walls than sun-leaves (Kürschner 2002; Milligan *et al.* 2021). For character coding, we simply distinguish between cell walls showing less than one sinusoidal period of oscillation (this type often intergrades with straight and rounded anticlinal walls) and cell walls showing more than one sinusoidal period of oscillation (Supporting Information, Appendix S1).

Ordination analysis

Cuticle samples were coded for 18 categorical characters described in Supporting Information, Appendix S1. These data were analysed in R v.4.3.1 (2023) using the 'vegan' package v.2.6-4 (Oksanen *et al.*, 2022), with all characters independent and equally weighted. Two dissimilarity matrices were produced from Bray–Curtis distances calculated among all 53 species surveyed (stress = 0.13) and only among the 34 surveyed species of *Schinus* (stress = 0.12), and the dissimilarity matrices were ordinated in three dimensions using nonmetric multidimensional scaling (NMDS). The *envfit* function was used to test for significant linear correlation between individual characters and regions of data points representing genera or species groups by a permutation test (alpha = 0.001), and to create character direction vectors in the 2D NMDS plot, showing their relationship to genera or species groups (polygons).

RESULTS

Descriptions

Euroschinus

Species observed (7 of 9): *E. elegans* Engl., *E. falcata*, *E. obtusifolia* Engl., *E. papuana*, *E. rubromarginata* Baker fil., *E. verrucosa* Engl., and *E. viellardii* Engl.

Description: Leaves are hypostomous. Outer stomatal ledges are level with the epidermal surface (Fig. 4A, B) or slightly sunken

showing cyclocytic subsidiary cells and unspecialized epidermal cells with straight anticlinal walls. Scale bar = 100 μm. F, adaxial surface of *S. terebinthifolia* showing simple acicular trichomes and cylindrical glands along a secondary vein; note the fine striations which ornament the cuticle surface. Scale bar = 100 μm. G, abaxial surface of *S. weinmannifolia* showing glands with a unicellular stalk and cylindrical bodies of 3–5 tiers. Scale bar = 100 μm. H, adaxial surface of *S. terebinthifolia* showing the base of a simple acicular trichome and epidermal cells with straight anticlinal walls. Scale bar = 100 μm.

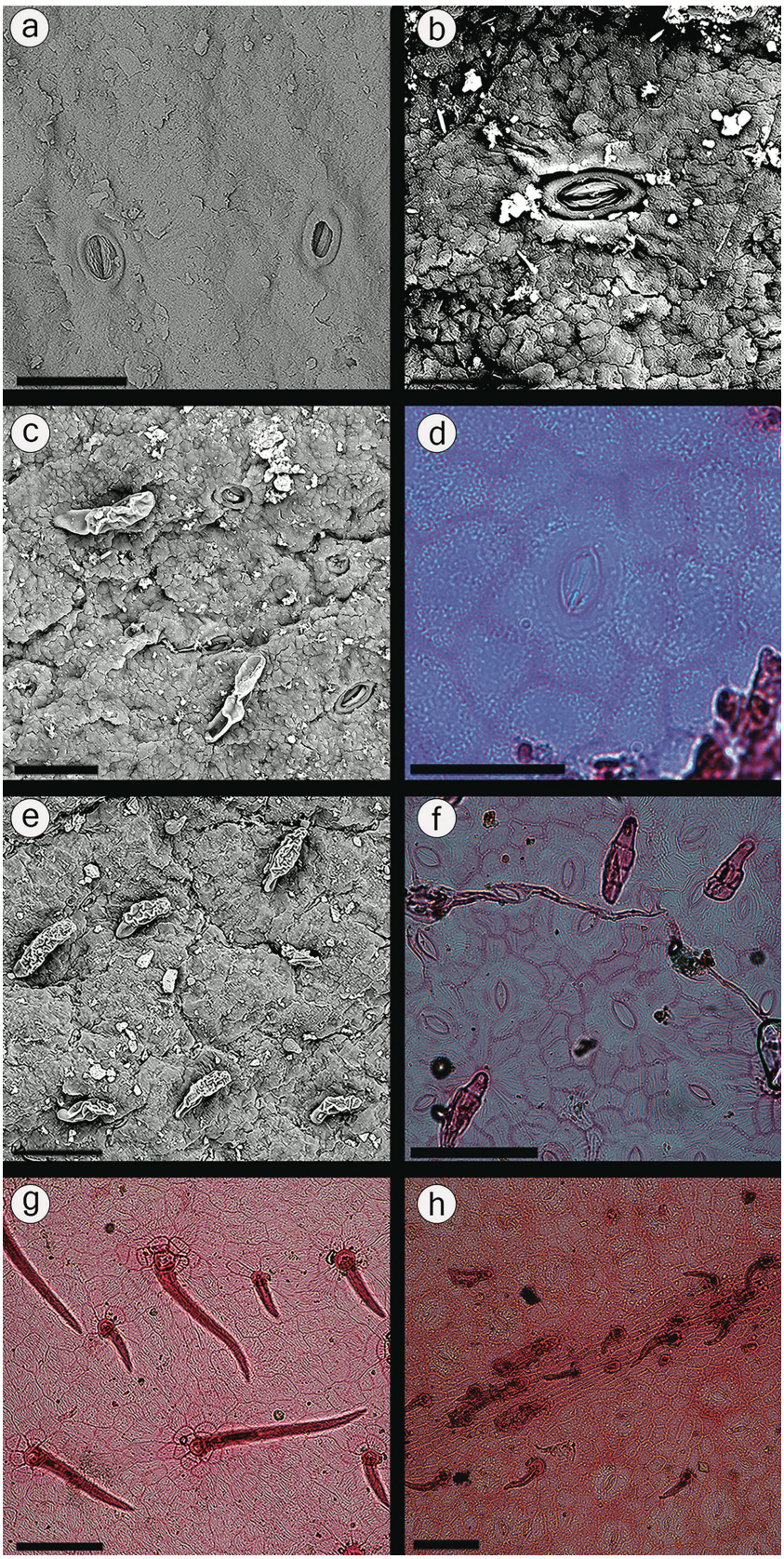

Figure 10. Cuticular features in *Schinus* section *Schinus*. A, SEM micrograph of the adaxial surface of *S. areira* showing stomatal complexes with level stomatal ledges and striated interior of the antechamber. Scale bar = 50 μm. B, abaxial surface of *S. molle* showing a stomatal complex with sunken stomatal ledges. Scale bar = 30 μm. C, abaxial surface of *S. molle* showing sunken stomata, cylindrical glands, and wax flakes. Scale bar = 50 μm. D, light micrograph of the abaxial surface of *S. areira* showing an anomocytic stomatal complex. Scale bar = 100 μm. E, adaxial surface of *S. molle* showing sunken stomata, glands, and cuticular ridges. Scale bar = 100 μm. F, abaxial surface of *S. molle* showing glands with unicellular stalks and uniseriate bodies with two or three tiers. Scale bar = 100 μm. G, adaxial surface of *S. molle* showing unspecialized epidermal cells with straight walls and rings of epidermal cells around trichome bases. Scale bar = 100 μm. H, adaxial surface of *S. areira* showing a cluster of simple acicular trichomes along the primary vein. Scale bar = 100 μm.

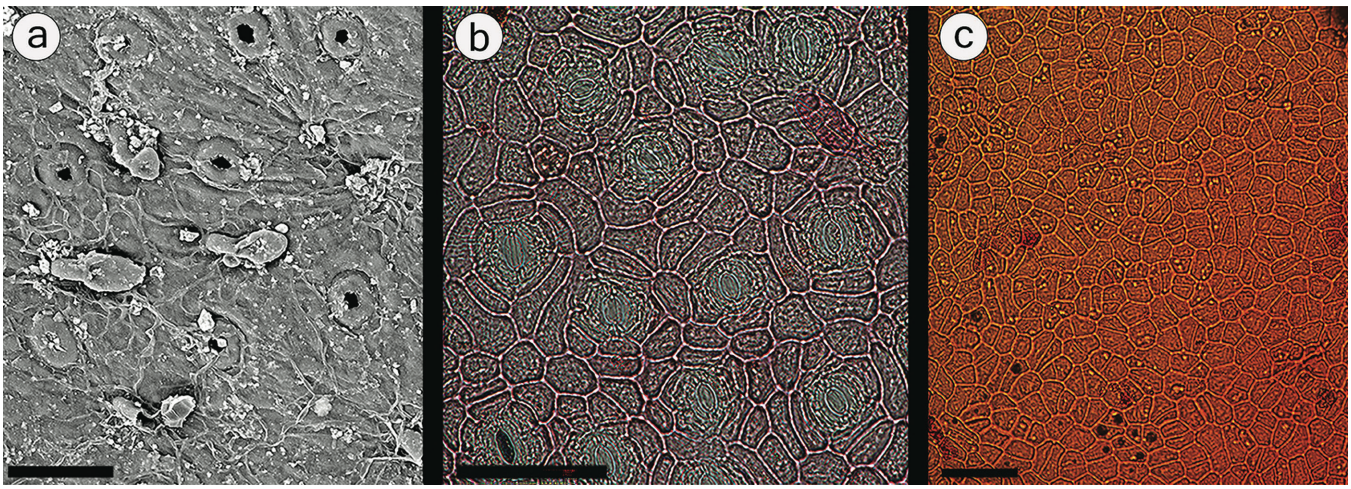

Figure 11. Cuticular features of *Schinus* section *Lentiscifolia*. A, abaxial surface of *S. lentiscifolia* showing stomatal complexes and glands. Scale bar = 50 μm. B, abaxial surface of *S. lentiscifolia* showing cyclocytic stomatal complexes and a gland. Scale = 100 μm. C, adaxial surface of *S. lentiscifolia* showing epidermal cells with straight or curved anticlinal walls. Scale bar = 100 μm.

(Fig. 4C, D). When sunken, a peristomatal rim may be level with the base of the outer stomatal ledges (Fig. 4C), or level with the epidermal surface (Fig. 5D); when level, the peristomatal rim is absent or poorly developed (Fig. 4A, B, E). Outer stomatal ledges are protruding, and the shape of the stoma may be broadly elliptical to roundish (Fig. 4B, D), or narrowly elliptical (Fig. 4E). Polar cutin bars (Fig. 4B, D) and circumstomatal striae (Fig. 4E) are variably present, the former being well-developed in *E. papuana*, and the latter in *E. rubromarginata* and *E. obtusifolia*. Stomatal complexes are anomocytic (Fig. 4F, G) or cyclocytic (Fig. 4H, I). The thickness of anticlinal walls of contact cells is variable, and they are not preserved in some samples (Fig. 4H). Walls of contact cells may be undulate or straight when adjacent, unspecialized epidermal cells have undulate cell walls (Fig. 4G, H).

Adaxial leaf surfaces are puberulent with glandular and simple trichomes while the abaxial surface is puberulent, glandular (Fig. 5A), or pubescent-glandular (Fig. 5C), and shallow axillary hairy tuft domatia occur in secondary vein axils of *E. falcata* (Fig. 5B). Simple trichomes are acicular (Fig. 5C). Acuminate-cylindrical glands (Figs 4C, G, 5A, D, E) occur on both surfaces and occasionally cluster in secondary vein axils (Fig. 5B). This gland type was observed in all species except for *E. elegans*, in which the apical cell is rounded rather than acute or acuminate (Fig. 5F). The cells adjacent to the stalks of glandular trichomes retain the shape and size of unspecialized epidermal cells (Fig. 5H, I).

Adaxial and abaxial epidermal cells have straight (Fig. 5G) or undulate walls (Fig. 5H, I); undulations may be wavy (Fig. 5I) or highly sinuous (Fig. 5H). Their periclinal walls are smooth (Fig. 4D) or ornamented with wax flakes (Fig. 5A) or striations (Fig. 5E). When ornamentation is present, it typically occurs on the abaxial surface. Radial and circumstomatal bands of striae are frequently associated with stomatal complexes (Figs 4C–E, 5D, F).

Lithrea

Species observed (3/3): *L. brasiliensis* Marchand, *L. caustica* Hook. & Arn., and *L. molleoides* (Vell.) Engl.

Description: Leaves are hypostomous. The base of outer stomatal ledges is level with the epidermal surface (Fig. 6A, B), or slightly sunken in *L. caustica* (Fig. 6C), and the ledges protrude from the epidermal surface, forming a cylindrical or dome-like antechamber. When outer stomatal ledges are level and completely encircled by a conspicuous peristomatal rim at the same height (Fig. 6A, B), thickenings on the periclinal walls of cyclocytic subsidiary cells may form a second ring encircling the stomatal ledges (Fig. 6A, C). When outer stomatal ledges are sunken, the peristomatal rim is also sunken or absent (Fig. 6C). Stomatal complexes are mainly cyclocytic (Fig. 6C–F) but occasional anomocytic (Fig. 6D, F) complexes are also present.

Adaxial and abaxial surfaces are puberulent with very sparse glandular and simple trichomes in *L. brasiliensis* and *L. molleoides*, while *L. caustica* is pubescent with simple trichomes covering the abaxial surface and densely distributed on the adaxial midvein (Fig. 6G, H). Acicular simple trichome bases are surrounded by one or two rings of 5–8 epidermal cells which are differentiated from unspecialized epidermal cells by having a cyclocytic arrangement (Fig. 6H). Glands are short-stalked and uniseriate (Fig. 6B).

Adaxial and abaxial epidermal cells have straight or slightly curved anticlinal walls (Fig. 6I, H). The periclinal wall of the epidermal cells is smooth (Fig. 6C) or covered in angular wax flakes (Fig. 6A, B).

Mauria

Species observed (9 of 16): *M. cuatrecasasii* F.A.Barkley, *M. denticulate* J.F.Macbr., *M. ferruginea* Tul., *M. heterophylla* Kunth., *M. peruviana* Cuatrec., *M. sericea* Loes., *M. simplicifolia* Kunth., *M. subserrata* Loes., and *M. thaumatophylla* Loes.

Description: Leaves are hypostomous (Fig. 7A). Outer stomatal ledges are protruding, and the base may be level with the epidermal surface (Fig. 7B, C) or slightly sunken (Fig. 7D, E). Stomatal ledges form a narrow, oval, or wide, oblong pore, and the interior antechamber is frequently striated (Fig. 8B–E); striations are particularly prominent in species with sunken stomatal ledges and may fill the entirety of the pore (Fig. 7E). A peristomatal rim is weakly developed in the stomatal complexes

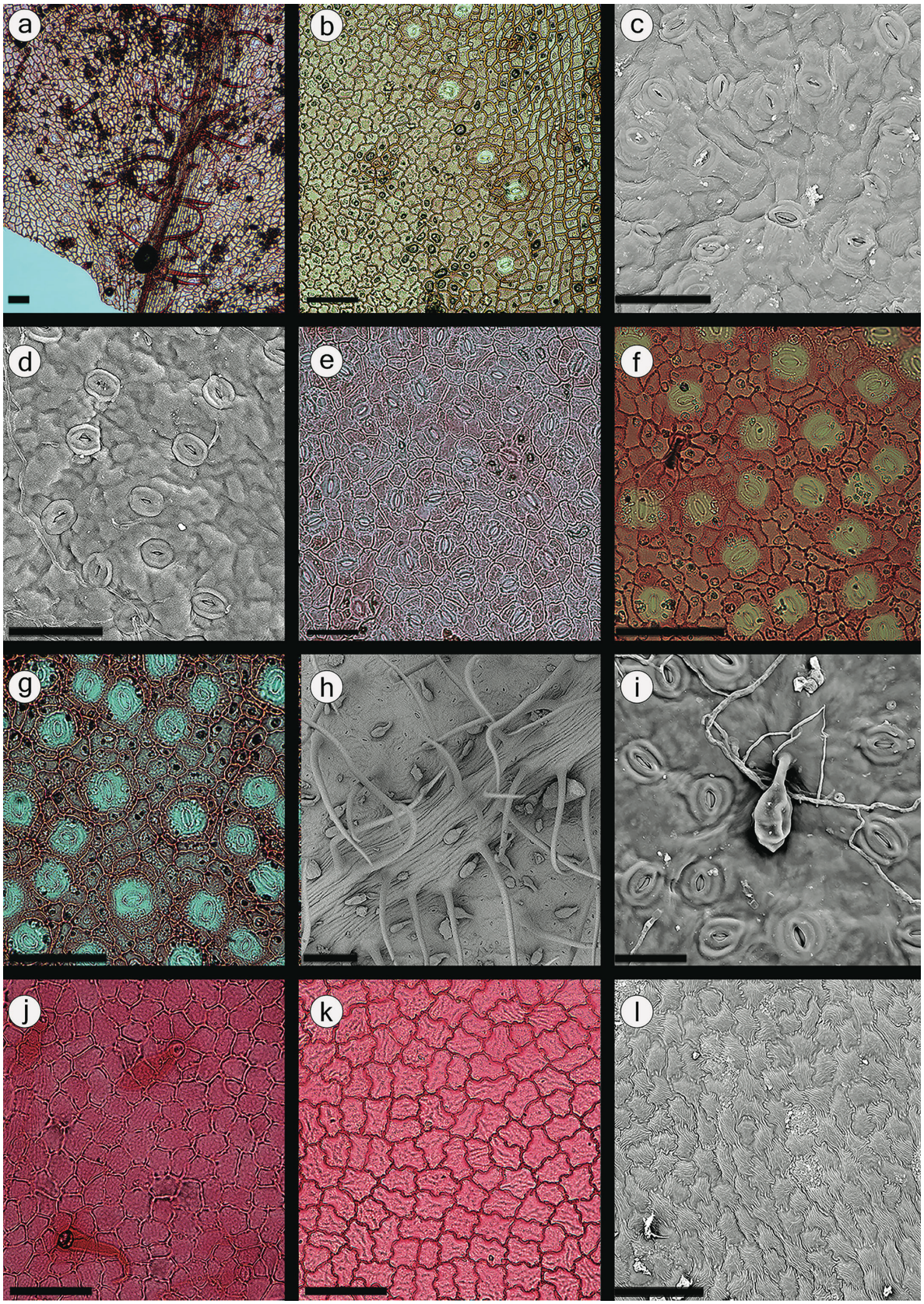

Figure 12. Cuticular features of *Schinus* section *Atlantica*. A, light micrograph of the adaxial surface of *S. spinosa* showing distribution of stomata and trichomes. Scale bar = 100 μm. B, adaxial surface of *S. ramboi* showing partial distribution of stomata. Scale bar = 100 μm. C, SEM micrograph of the abaxial surface of *S. longifolia* showing stomatal complexes with protruding cuticular ledges and a peristomal ring. Scale bar = 50 μm. D, abaxial surface of *S. ramboi* showing stomata. Scale bar = 50 μm. E, abaxial surface of *S. longifolia* showing anomocytic stomatal complexes. Scale bar = 100 μm. F, abaxial surface of *S. engleri*. Scale bar = 50 μm. G, abaxial surface of *S. ramboi* showing cyclocytic stomatal

where stomatal ledges are level with the epidermal surface (Fig. 7B, C), and conspicuous in those with sunken stomatal ledges (Fig. 7D, E). Subsidiary cells are cyclocytic or anomocytic (Fig. 7D–G) and may exhibit cuticular thickening on the periclinal wall (Fig. 7D, E).

Indumentum of the abaxial surface is puberulent, glandular (Fig. 7H), or pubescent-glandular (Fig. 7I), and hairy tuft domatia are frequently present in secondary vein axils (Fig. 7K, L). Indumentum of the adaxial surface is glabrous to puberulent (Fig. 8F), or pubescent (Fig. 7J). Simple trichomes are acicular, ribbon-like, or conical, and multiple types often occur together in tuft domatia (Fig. 7K, L). Glands are cylindrical or ovoid (Fig. 7B, C). Cylindrical glands are uniseriate and attached to long, unicellular stalks (Figs 7H, 8B, D–E) whereas ovoid glands are uniseriate or multiseriate, and attached to short stalks that widen at the attachment point with the gland (Fig. 8C). The bases of glands are surrounded by 5–9 unspecialized epidermal cells (Fig. 8G) or radially elongated cells (Fig. 8D). Simple trichome bases are surrounded by unspecialized epidermal cells or 1–3 rings of cyclocytic cells.

Epidermal cell anticlinal walls are straight or curved on both sides of the leaf (Fig. 8D, E, G, H). Leaf surfaces lack ornamentation but sometimes have a reticulate braided texture which is inferred to result from cuticle deposition along anticlinal walls of epidermal cells (Fig. 8F).

Schinus section *Terebinthifolia*

Species observed (2/2): *S. terebinthifolia* Raddi and *S. weinmannifolia* Engl.

Description: Leaves are hypostomous (*S. terebinthifolia*) or amphistomous (*S. weinmannifolia*) with adaxial stomata distributed adjacent to veins and the margin (Fig. 9A). Stomatal ledges are level with the epidermal surface and are flat or slightly protruding (Fig. 9B, C); a striate peristomatal rim is present in *S. terebinthifolia* while it is weakly developed or absent in *S. weinmannifolia* (Fig. 9B, C). Stomatal complexes are cyclocytic and contain 5–7 subsidiary cells (Fig. 9D, E).

Glandular and simple trichomes are distributed on both leaf surfaces, along primary and secondary veins in *S. terebinthifolia*, and scattered in *S. weinmannifolia* (Fig. 9F, G). Simple trichomes are acicular, and their base is encircled by 1-3 rings of epidermal cells (Fig. 9H). Gladular hair stalks are unicellular and or rarely bicellular (Fig. 9F, G) and are surrounded by 5–8 slightly wedge-shaped epidermal cells (Fig. 9E); the glands are cylindrical and multiseriate with 3–5 tiers of cells. Epidermal cells have straight or rounded anticlinal walls (Fig. 9E, H). Leaf surfaces are smooth or ornamented with densely packed bands of fine cuticular striae in *S. terebinthifolia* (Fig. 9B, F).

Schinus section *Schinus*

Species observed (2/2): *S. areira* L. and *S. molle* L.

Description: Leaves are amphistomous. Stomatal complexes have protruding stomatal ledges that are level with the epidermal surface and lack a peristomatal rim (Fig. 10A), or have protruding stomatal ledges that are sunken, and have a peristomatal rim that is level with the epidermal surface (Fig. 10B, C). The interior of the antechamber is ornamented with fine striae, and the shape of the stoma is oval or oblong (Fig. 10A, B). The anticlinal walls of contact cells are thin and often not preserved after cuticles are cleared; the configuration of contact cells appears to be anomocytic or cyclocytic (Fig. 10D, F).

Adaxial and abaxial surfaces are puberulent (Fig. 10E–H). Simple acicular trichomes occur in clusters along primary veins on both surfaces and are sparsely scattered elsewhere (Fig. 10G, H); their bases are surrounded by one or two rings of cyclically arranged epidermal cells (Fig. 10G). Glands are born on unicellular stalks, are cylindrical, uniseriate, and consist of 3–5 tiers; stalks are surrounded by 5–7 epidermal cells (Fig. 10E, F).

Epidermal cell walls are straight or rounded on both surfaces (Fig. 10F, G). Abaxial and adaxial surfaces are ornamented with wax flakes (Fig. 10A, B); the cuticular surface may develop ridges in *S. molle*, and stomata are often found in the 'valleys' of the resulting topography (Fig. 10C, E).

Schinus section *Lentiscifolia*

Species observed (1/1): *S. lentiscifolia* Marchand.

Description: Leaves are amphistomous. Outer stomatal ledges are flat and their base is level with the epidermis; a peristomatal rim is absent (Fig. 11A). Stomatal complexes are cyclocytic with 5–7 subsidiary cells (Fig. 11B). Adaxial and abaxial surfaces are puberulent (nearly glabrous); simple trichomes and glands are extremely sparse. Glandular trichomes are composed of a unicellular stalk and an ovoid gland (Fig. 11A). Epidermal cell anticlinal walls are straight on both surfaces (Fig. 11B, C).

Schinus section *Atlantica*

Species observed (5/5): *S. engleri* F.A.Barkley, *S. ferox* Hassl., *S. longifolia* (Lindl.) Speg., *S. ramboi* F.A.Barkley, and *S. spinosa* Engl.

Description: Leaves are hypostomous (*S. engleri* var. *engleri*, *S. ferox*) or partially amphistomous (*S. longifolia*, *S. ramboi*, *S. spinosa*; Fig. 12A, B). Outer stomatal ledges are protrusive and level with the epidermal surface at the base; stomatal pore shape

complexes. Scale bar = 100 μm. H, abaxial surface of *S. ferox* showing simple trichomes and glands. Scale bar = 200 μm. I, abaxial surface of *S. engleri* showing a short-stalked, ovoid gland. Scale bar = 30 μm. J, adaxial surface of *S. ferox* showing a simple trichome base and a gland base. Scale bar = 100 μm. K, adaxial surface of *S. engleri* showing epidermal cells with wavy anticlinal walls. Scale bar = 100 μm. L, adaxial surface of *S. longifolia* showing fine striations and wavy anticlinal walls. Scale bar = 100 μm.

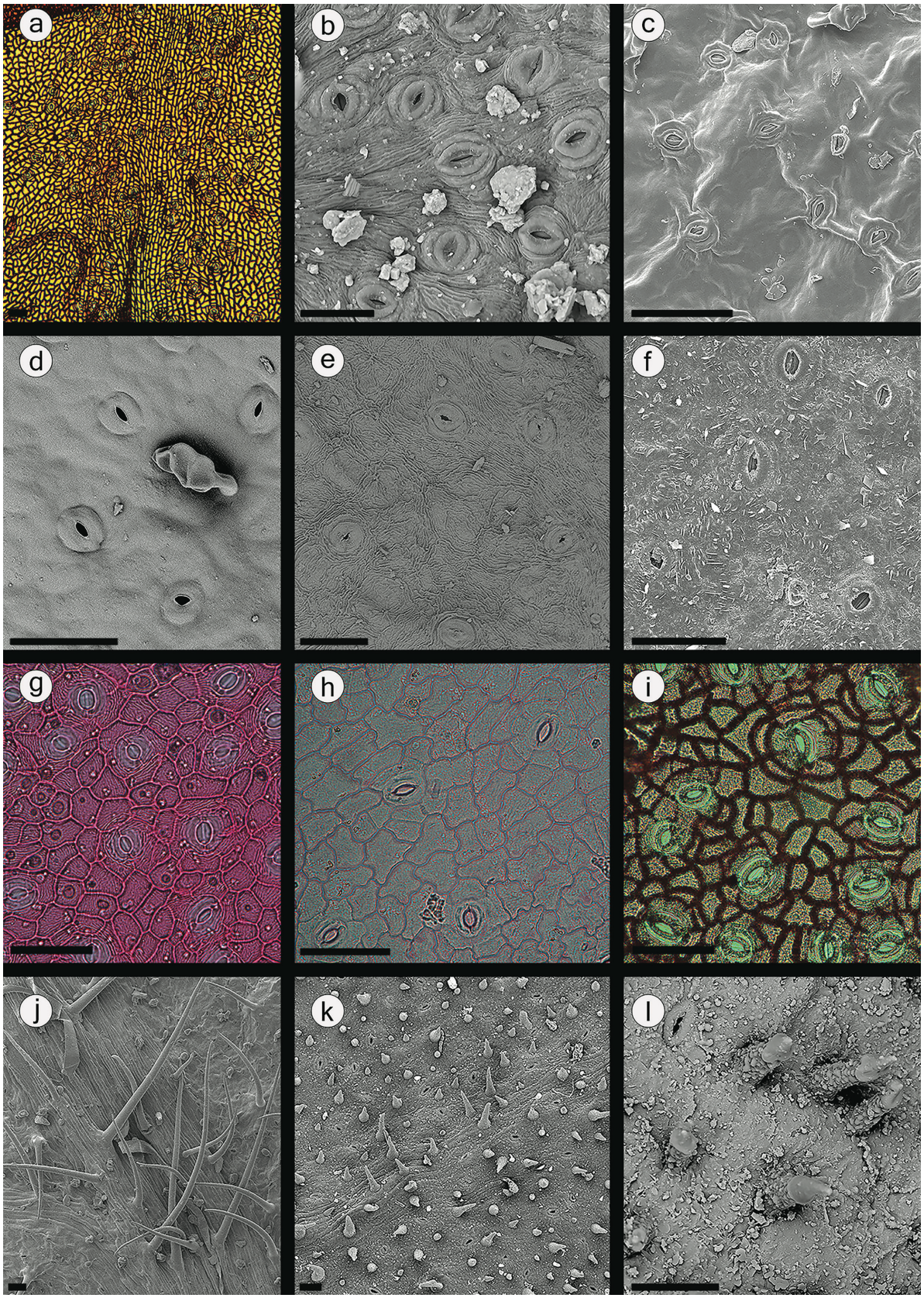

Figure 13. Cuticular features of *Schinus* section *Pilifera*. A, light micrograph of the adaxial surface of *S. pilifera* var. *boliviensis* showing stomata clustered along the midrib and simple trichomes. Scale bar = 100 μm. B, SEM micrograph showing abaxial surface of *S. pilifera* showing striate ornamentation and stomatal complexes with protruding stomatal ledges. Scale bar = 30 μm. C, abaxial surface of *S. pearcei* showing cuticular ridges and stomata. Scale bar = 50 μm. D, adaxial surface of *S. engleri* var. *uruguayensis* showing stomatal complexes without peristomal rings and flat stomatal ledges. Scale bar = 30 μm. E, abaxial surface of *S. bumelioides* showing striae and stomata. Scale bar = 50 μm. F, abaxial surface of *S. praecox* showing wax flakes and stomata. Scale bar = 50 μm. G, abaxial surface of *S. bumelioides* showing anomocytic stomatal complexes

is oval to fusiform; a peristomal ring is present and smooth (Fig. 12C, D). Stomatal complexes include 4–7 contact cells and are anomocytic (Fig. 12E), anomocytic and cyclocytic (Fig. 12F), or entirely cyclocytic (Fig. 12G).

Leaf surfaces are puberulent except for the abaxial surfaces of *S. ferox* and *S. spinosa* in which glandular trichomes occur densely over the surface while simple trichomes cluster along major veins (Fig. 12H). Glandular trichomes have unicellular stalks and ovoid to cylindrical glands; glands are uniseriate or multiseriate and consist of 1–3 tiers (Fig. 12H, I); stalks are surrounded by five or more wedge-shaped epidermal cells. Simple trichomes are acicular, and their bases are surrounded by five or more epidermal cells (Fig. 12J).

Anticlinal walls are rounded or undulate and have similar shapes on each leaf surface in individual species (Fig. 12J–L); anticlinal wall undulations are most pronounced in the adaxial epidermis of *S. engleri* and *S. longifolia* but also occur in abaxial epidermal cells of these species. Leaf surfaces are often smooth; dense, fine striae that cover individual epidermal cells may develop on the adaxial surface in *S. longifolia* (Fig. 12L), and circumstomatal striae are present in *S. ferox* (Fig. 12H).

Schinus section *Pilifera*

Species observed (7/7): *S. bumelioides* I.M.Johnst., *S. fasciculata* (Griseb.) I.M.Johnst., *S. johnstonii* F.A.Barkley, *S. pearcei* Engl., *S. pilifera* I.M.Johnst., *S. praecox* (Griseb.) Speg., and *S. sinuate* (Griseb.) Engl.

Description: Leaves are amphistomous with approximately equal stomatal densities on each surface (*S. bumelioides*, *S. engleri* var. *uruguayensis*, *S. johnstonii*, *S. pearcei*, *S. enturi*) or partially amphistomous (*S. fasciculata*, *S. praecox*, *S. pilifera*; Fig. 13A), with adaxial stomata less dense than abaxial stomata and aggregated only along the midrib. Outer stomatal ledges are flat or protruding and level with epidermal cells at the base (Fig. 13B–D). A peristomal rim is absent (Fig. 13D–F) or present and contiguous with stomatal ledges (Fig. 13B, C), striate in *S. fasciculata* and *S. pilifera* (Fig. 13B). Circumstomatal striae encircle the stomatal complex in *S. bumelioides* but do not form a well-defined ring (Fig. 13E). Stomatal complexes have 4–7 contact cells and are anomocytic (Fig. 13G, H) or cyclocytic (Fig. 13I).

Indumentum is pubescent-glandular (Fig. 13J), pubescent, or puberulent; simple trichomes are denser and more widely distributed on abaxial surfaces in species with pubescent-glandular indumentum (*S. pilifera*, *S. fasciculata*). In *S. johnstonii*, both surfaces are densely covered by distinctive short conical, simple trichomes which may develop an apical wax cap (Fig. 13J, K) and their base is sometimes thickened and surrounded by 5–7 epidermal cells (Fig. 14A). Simple acicular trichome bases are surrounded by 5–7 epidermal cells (Fig. 14B). Glandular trichomes have short, unicellular stalks surrounded by 5–7 radially elongated epidermal cells; glands are ovoid or cylindrical, (Fig. 16C-F) and uniseriate (1–3 tiers), unicellular or multicellular (Figs 13D, 14C–F).

Cell anticlinal wall shape ranges from straight to rounded in *S. bumelioides* (Fig. 13G), *S. praecox*, and *S. pearcei*, from straight to undulate in *S. pilifera* (Figs 13A, I, 14B, E), and from rounded to undulate in *S. fasciculata* and *S. enturi* (Fig. 13H); anticlinal cell wall shape is consistent between cells on opposite surfaces of an individual leaf. Leaf surfaces are ornamented with fine striae that form large continuous bands (Figs 13B, E, 14C) or with coarse wax flakes (Fig. 13F, L), with one feature occurring to the exclusion of the other. Undulations in the cuticle create conspicuous microtopographical relief on the abaxial surfaces of *S. sinuata* and *S. pearcei* (Fig. 14D, F).

Schinus section *Montana*

Species observed (5 of 6): *S. marchandii* F.A.Barkley, *S. montana* (Phil.) Engl., *S. odonellii* F.A.Barkley, *S. patagonica* (Phil.) I.M.Johnst. ex Cabrera, and *S. roigii* Ruiz Leal & Cabrera.

Description: Leaves are hypostomous (*S. montana*, *S. patagonica*) or amphistomous (*S. marchandii*, *S. odonellii*, *S. roigii*). Outer stomatal ledges are flat and sunken (Fig. 15A, B), flat and level with the epidermal surface at their base (Fig. 15C), or protruding and level with the epidermal surface at their base (Fig. 15D, E). The peristomatal rim is absent (Fig. 15A–E). Stomatal complexes have 5–9 contact cells, and their configuration variably appears anomocytic (Fig. 15F, G) and cyclocytic with guard cells surrounded by one or more rings of subsidiary cells (Fig. 15H).

Adaxial and abaxial surfaces are glabrous to puberulent, and the occurrence of simple trichomes or glands is sparse. Indumentum is only a notable feature in *S. odonellii* where simple acicular trichomes may cluster along the midvein and cutin ridges (Fig. 15I, J). The base of simple trichomes is surrounded by 5–8 cells which are not distinguished from unspecialized epidermal cells (Fig. 15K). Glandular trichomes are sparse on both surfaces in all species; their stalks are unicellular, and glands are cylindrical and uniseriate, often three-tiered (Fig. 15L).

Anticlinal walls of epidermal cells are straight or rounded on the abaxial surface (Fig. 15G, F) and straight, rounded, or slightly undulate on the adaxial surface (Fig. 16A, B). Cuticular surfaces may be smooth (Fig. 15A), striate (Figs 15E, 16C), or ornamented with angular wax flakes (Fig. 15B, C). Both striations and wax flakes may be present on an individual but do not commonly occur on the same surface; striations appear more prominently on the adaxial surface (Fig. 16C) and wax flakes on the abaxial surface (Fig. 16B, C). Cuticular ridges are a prominent feature of *S. odonellii* (Fig. 16I).

Scale bar = 100 μm. H, adaxial surface of *S. sinuata* showing anomocytic stomatal complexes. Scale bar = 100 μm. I, abaxial surface of *S. pilifera* showing cyclocytic stomatal complexes. Scale bar = 100 μm. J, abaxial surface of *S. pilifera* var. *cabrerae* showing the distribution of simple trichomes along the midrib. Scale bar = 300 μm. K, abaxial surface of *S. johnstonii* showing simple, conical trichomes Scale bar = 200 μm. L, adaxial surface of *S. johnstonii* showing conical trichomes with a wax cap. Scale bar = 50 μm.

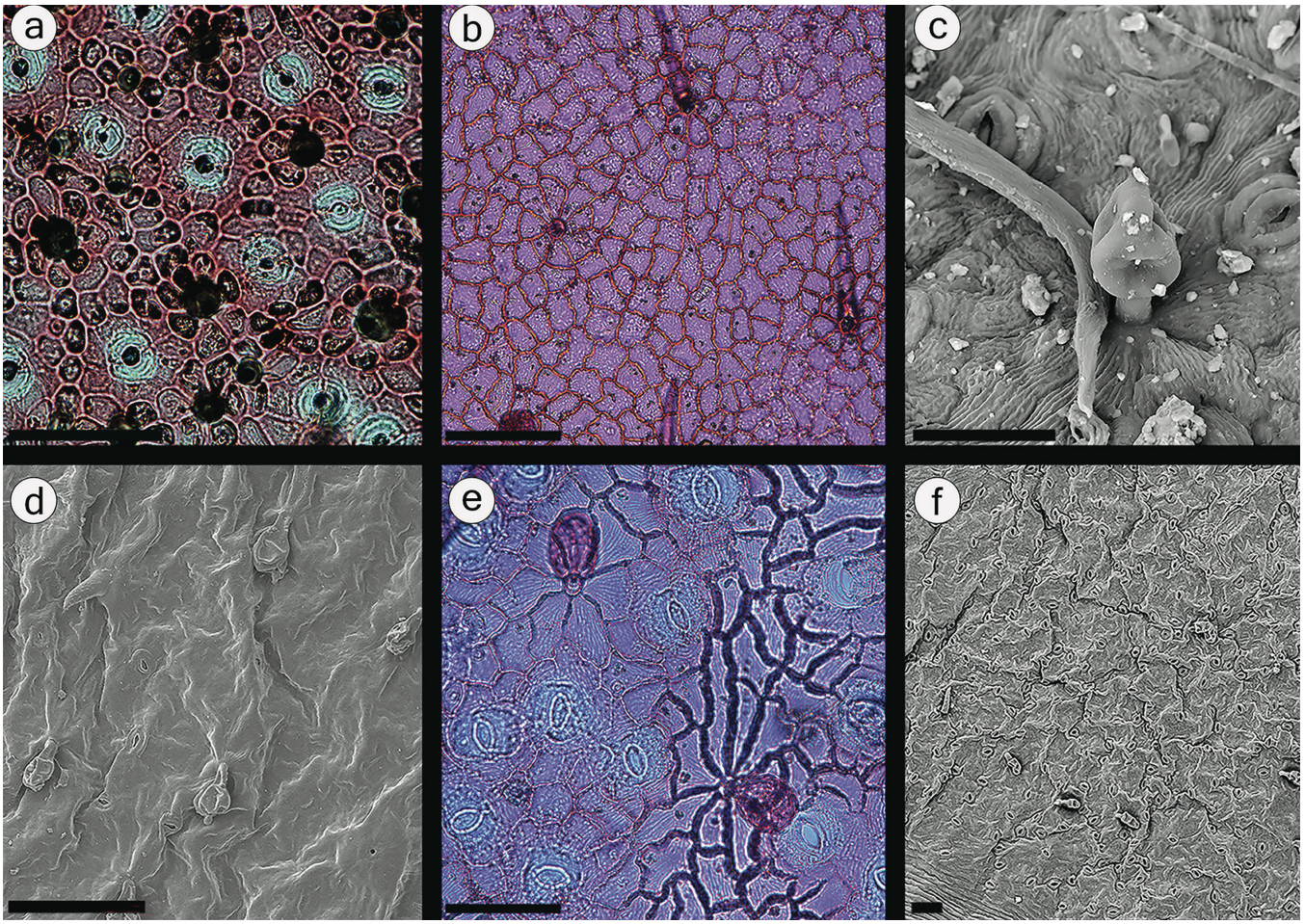

Figure 14. Cuticular features of *Schinus* section *Pilifera*. A, abaxial surface of *S. johnstonii* showing the base of conical trichomes and stomatal complexes. Scale bar = 100 μm. B, adaxial surface of *S. pilifera* var. *cabrerae* showing epidermal cells with curved anticlinal walls and trichome bases. Scale bar = 100 μm. C, abaxial surface of *S. pilifera* showing a short-stalked, ovoid gland. Scale bar = 30 μm. D, adaxial surface of *S. pearcei* showing cuticular ridges and deflated ovoid glands. Scale bar = 100 μm. E, abaxial surface of *S. pilifera* var. *cabrerae* showing gland bases. F, abaxial surface of *S. sinuate* showing cuticular ridges and short-stalked cylindrical trichomes Scale bar = 50 μm.

Schinus section Duvaua

Species observed (3/3): S. latifolia (Gillies ex Lindl.) Engl., *S. velutina* (Turcz.) I.M.Johnst., and *S. polygama* (Cav.) Cabrera.

Description: Leaves are amphistomous or partially amphistomous (Fig. 17A–C); the distribution of stomata on the adaxial surface is less dense than on the abaxial surface and may be spatially restricted to the midvein (Fig. 17A), or to the midvein and major veins (Fig. 17C). The base of stomatal ledges is level with the epidermal surface and the ledges may be flat (Fig. 17D) or protruding (Fig. 18E–G); protruding stomatal ledges are encircled by a peristomatal rim that can be contiguous (Fig. 17F) or not contiguous (Fig. 17G) to the stomatal ledges. Stomatal complexes are associated with radial bands of striae in *S. latifolia* (Fig. 17G) and with circumstomatal striae in *S. polygama* var. *parviflora* (Fig. 17D). The occlusive (guard) cells are encircled by 5–7 cyclocytic subsidiary cells (Fig. 17G–I).

Leaf surfaces are glabrous to puberulent or covered in a dense indumentum of simple, acicular trichomes and sparse glands in *S. velutina* (Fig. 17A, I, K). Acicular trichomes are surrounded by one or multiple rings of epidermal cells with slightly thickened anticlinal walls (Fig. 17I, K). Glandular trichomes have unicellular stalks and ovoid or globose glands (Fig. 17J).

Adaxial epidermal cell anticlinal walls are rounded (Fig. 17B) or undulate (Fig. 17K, L) while those of the abaxial surface are rounded or undulate; the undulations have a shorter period and greater amplitude than on the adaxial surface (Fig. 17H, I). Adaxial and abaxial surfaces may be covered in dense bands of fine striations (Fig. 17L).

Schinus section *Myrtifolia*

Species observed (7 of 11): S. congestiflora Silva-Luz & Pirani, *S. gracilipes* I.M.Johnst., *S. meyeri* F.A.Barkley, *S. microphylla* I.M.Johnst., *S. minutiflora* Silva-Luz & Pirani, *S. myrtifolia* (Griseb.) Cabrera, and *S. venturii* F.A.Barkley.

Description: Leaves are hypostomous or amphistomous (only *S. microphylla*). Outer stomatal ledges are level with the epidermal surface and protrude to form an oval or oblong gape (Fig. 18A–D). A striate peristomal ring encircles the outer stomatal ledges (Fig. 18A, B); the ring is absent or weakly developed in *S. microphylla* (Fig. 18D). The interior antechamber

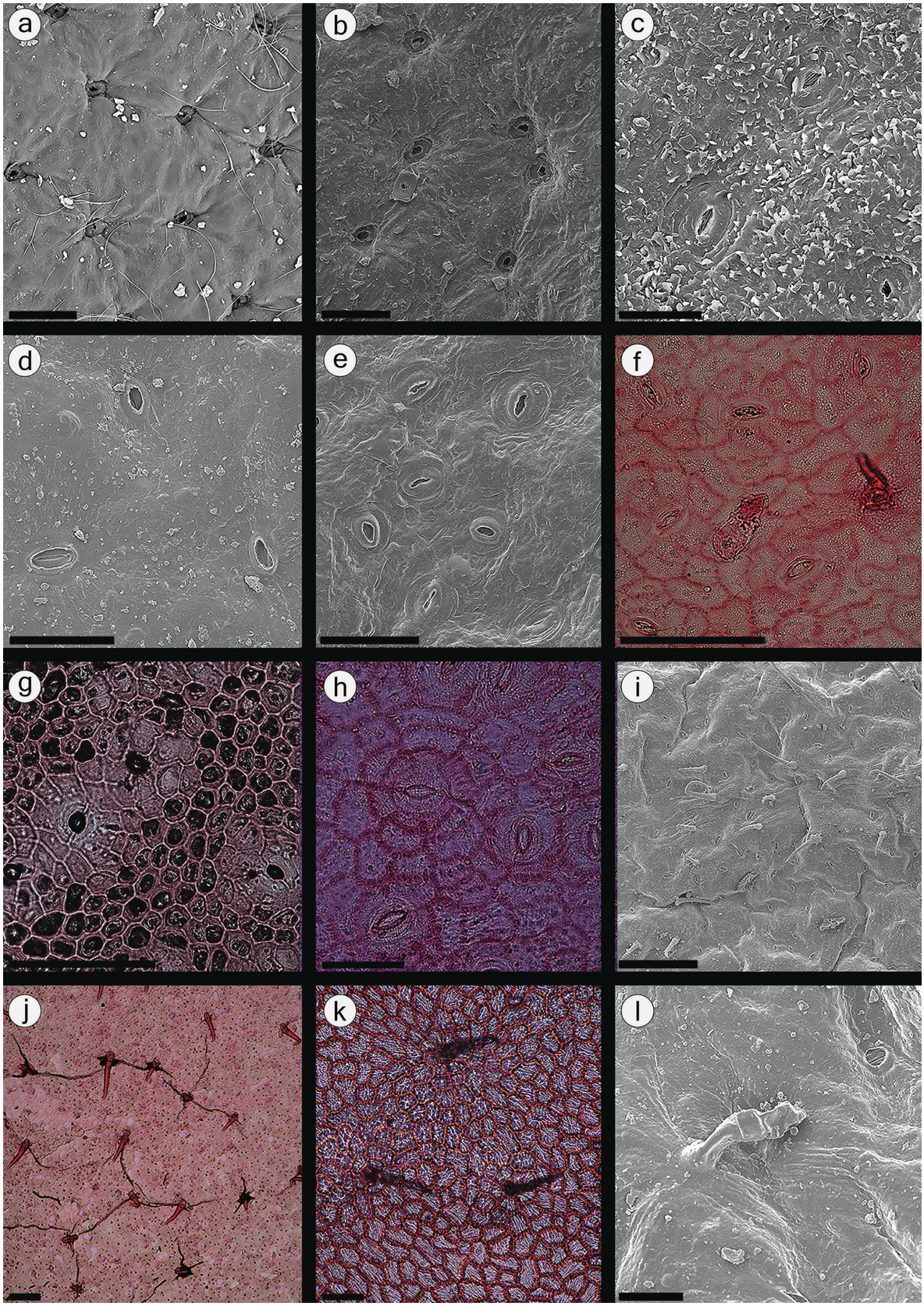

Figure 15. Cuticular features of *Schinus* section *Montana*. A, abaxial surface of *S. roigii* showing sunken stomata with flat stomatal ledges. Scale bar = 50 μm. B, abaxial surface of *S. marchandii* showing sunken stomata with flat cuticular ledges. Scale bar = 50 μm. C, abaxial surface of *S. montana* showing stomatal complexes level with the epidermal surface and having flat cuticular ledges; note wax flakes. Scale bar = 30 μm. D, adaxial surface of *S. odonellii* showing stomatal complexes with protruding cuticular ledges level with the epidermal surface at the base. Scale bar = 50 μm. E, abaxial surface of *S. montana* showing stomatal complexes and cuticular striae. Scale bar = 50 μm. F, abaxial surface of *S.*

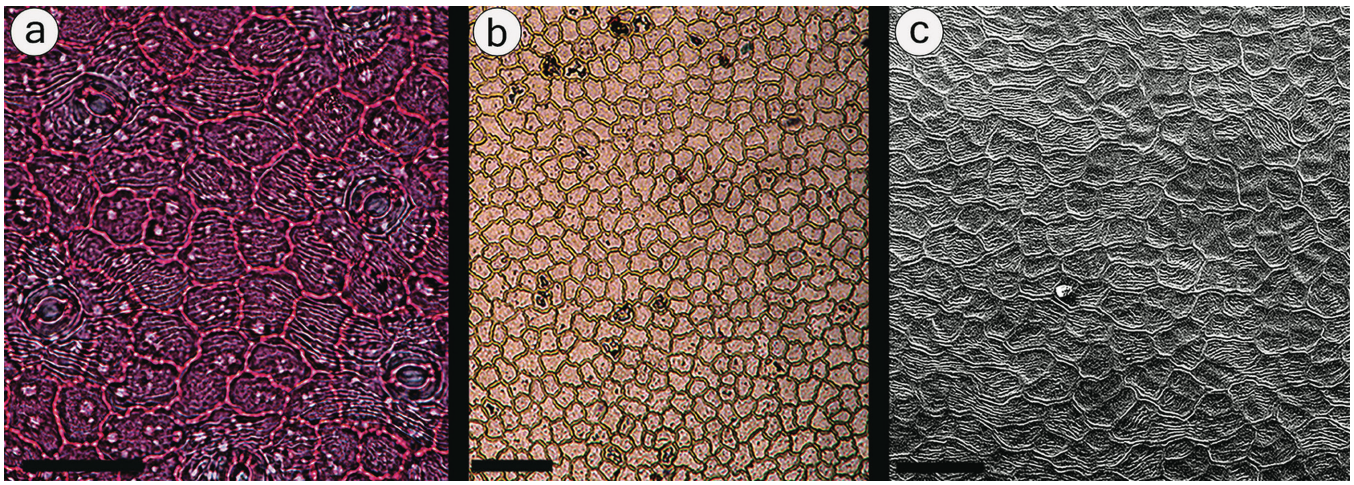

Figure 16. Epidermal cell shape and cuticular ornamentation in *Schinus* section *Montana*. All scale bars = 100 μm. A, adaxial surface of *S. marchandii* showing stomata and epidermal cells with curved and undulate (type 1) anticlinal walls. B, adaxial surface of *S. montana* showing epidermal cells with curved and undulate anticlinal walls. C, adaxial surface of *S. montana* showing cuticular thickenings of anticlinal walls and a striate surface.

is conspicuously striate (Fig. 18A, B). Stomatal complexes are cyclocytic with 5–7 subsidiary cells (Fig. 18F–H).

Leaf surfaces are mainly glabrous or puberulent (Fig. 18I); abaxial surfaces of *S. congestiflora* are pubescent with densely clustered glands (Fig. 18J). Simple trichomes are acicular. Glandular trichomes have a unicellular stalk and multiseriate, and ovoid or oblong glands of 2–3 tiers of cells. The stalks are surrounded by 5–8 epidermal cells which may be wedge-shaped (Fig. 18G) or resemble unspecialized epidermal cells (Fig. 18F, L). Adaxial epidermal cell walls are straight, rounded, or undulate Type 1 (Fig. 19A–C). Abaxial epidermal cells are straight, rounded, or undulate (Fig. 19D, E). Adaxial and abaxial surfaces are prominently striated with striations clustered in dense bands that span over multiple cells and may encircle stomatal complexes (Fig. 19F). Cuticular ridges are prominent on the abaxial surface in *S. congestiflora* and *S. microphylla* (Fig. 19D, E, J).

NMDS ordination

Ordination of all 53 surveyed species on the first two axes of variation produces two overlapping pairs in which species of *Schinus* and *Lithrea* occupy relatively positive values on NMDS 1 and *Euroschinus* and *Mauria* occupy relatively negative values on NMDS 1 (Fig. 20A). In a three-dimensional plot (Supporting Information, Appendix S2), *Mauria* and *Euroschinus* separate along the vertical dimension (NMDS 3), but *Schinus* and *Lithrea* remain overlapping. Ordination of all 34 surveyed *Schinus* species (Fig. 20B) illustrates that species groups within *Schinus* do not discriminate on two or three axes of variation (Appendix S2). Characters with significant linear correlation to genera ($P < .001$) were plotted as vectors on the 2D NMDS plots depicting cuticular variation among genera (Fig. 20C), and among sections of *Schinus* (Fig. 20D). Character vectors point in the direction of ordination space to which they are most strongly correlated, and vector magnitude is scaled to reflect the value of the r^2 correlation coefficient. In Fig. 20C, 11 of 18 total characters are significantly correlated with regions of the ordination plot: acuminate-cylindrical glands (Gl_T3), tuft domatia (Tu_Dom), long-stalked, cylindrical glands (Gl_T1), peristomal ring (PR), cuticular striae (Cut_str), adaxial anticlinal wall undulation (Ad_AW), short-stalked, ovoid glands (Gl_T4), outer stomatal ledge position (OSL_pos), stomatal distribution (Stom_dist), outer stomatal ledge shape (OSL_shp), and cuticular wax flaked (Cut_wax). However, only two characters, cuticular wax platelet presence–absence (Cut_wax) and peristomal ring presence–absence (PR) have r^2 values >.5. Interestingly, some characters which are clearly distinctive from a descriptive standpoint do not receive strong statistical support for discrimination between genera (e.g. acuminate-cylindrical glands were only observed in *Euroschinus* but $r^2 = .19$, and $P = .007$) while others which are descriptively more temperamental (e.g. cuticular wax platelets) received strong statistical support ($r^2 = .55$; $P = .001$). In Fig. 20D, seven of 18 characters are significantly correlated with regions of the ordination plot: Cut_wax, Cut_str, short-stalked ovoid glands (Gl_T2), Gl_T4, OSL_pos, OSL_shp, and PR.

odonellii showing anomocytic stomatal complexes and a simple, acicular trichome. Scale bar = 100 μm. G, abaxial surface of *S. roigii* showing an anomocytic stomatal complex and epidermal cells with straight anticlinal walls. Scale bar = 100 μm. H, abaxial surface of *S. patagonica* showing a cyclocytic stomatal complex with two rings of subsidiary cells. Scale bar = 100 μm. I, adaxial midrib of *S. odonellii* with simple, acicular trichomes; note cuticular ridges away from the midrib. Scale bar = 200 μm. J, abaxial surface of *S. odonellii* showing a cluster of simple trichomes occurring away from major veins; trichome bases are connected by a cuticular ridge. Scale bar = 100 μm. K, adaxial surface of *S. montana* showing simple trichomes surrounded by unspecialized epidermal cells with straight anticlinal walls. L, abaxial surface of *S. odonellii* showing a cylindrical gland with a unicellular stalk. Scale bar = 30 μm.

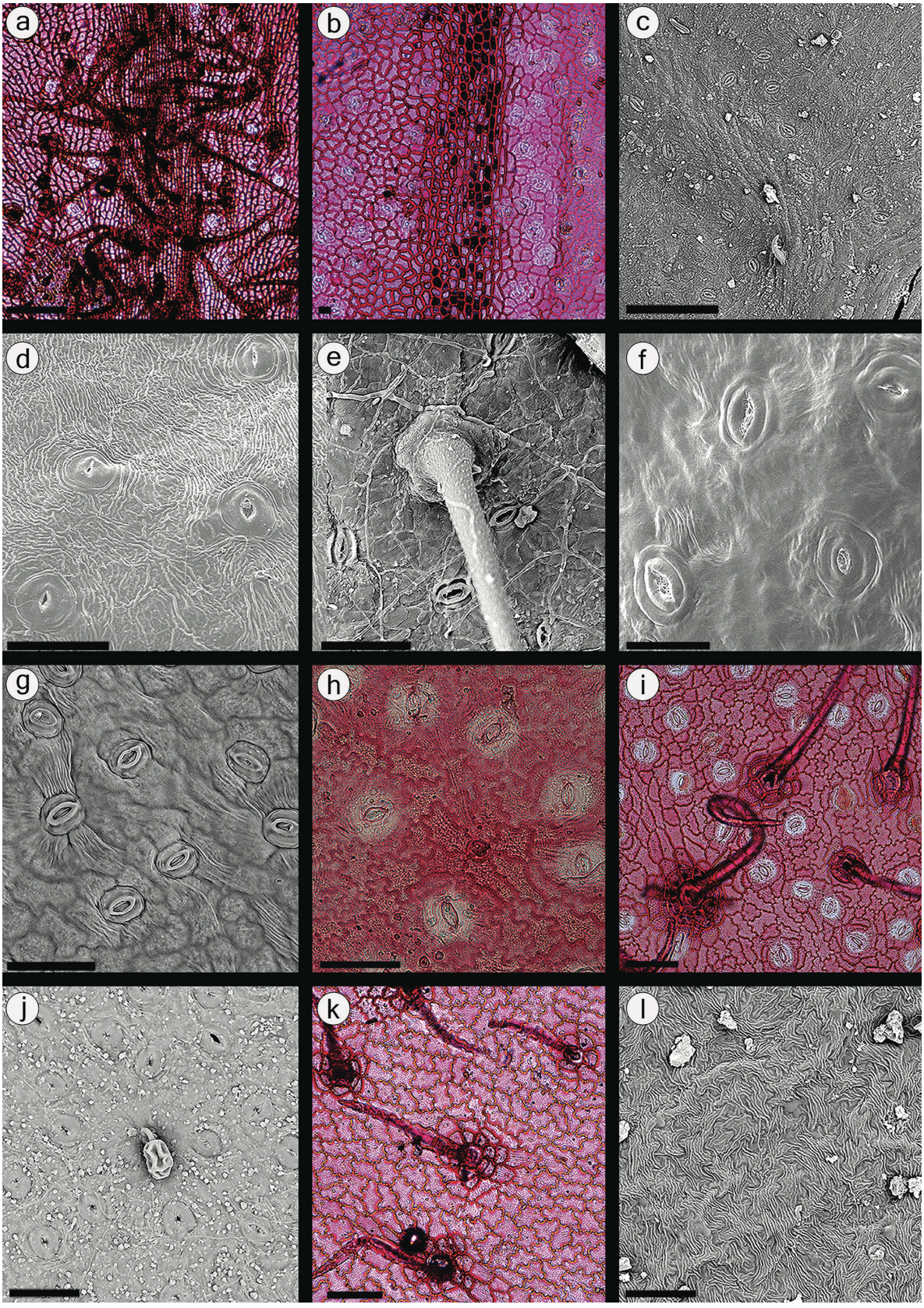

Figure 17. Cuticular features of *Schinus* section *Duvaua*. A, light micrograph of the adaxial midrib of *S. velutina* showing pilose vestiture and stomata with a restricted distribution. Scale bar = 100 μm. B, cleared cuticle of *S. polygama* showing marginal epidermal cells and the adaxial (left) and abaxial (right) surfaces. Scale bar = 100 μm. C, SEM micrograph of the adaxial surface of *S. latifolia* showing stomata distributed along a secondary vein. Scale bar = 200 μm. D, adaxial surface of *S. polygama* var. *parviflora* showing stomatal complexes with flat or barely protruding stomatal ledges and dense bands of striae. Scale bar = 50 μm. E, abaxial surface of *S. velutina* showing stomatal complexes with

DISCUSSION

Cuticular traits in Anacardiaceae

The cuticular characters observed in this study fall within the range of variation known to exist in the Anacardiaceae (Wilkinson 1971, 1979; Pell *et al.* 2011) but expand the range of morphologies known at lower taxonomic levels.

Hypostomous stomatal distribution is the most common type among all studied Anacardiaceae species and characterizes *Euroschinus*, *Lithrea*, *Mauria*, and some species in *Schinus* sections *Terebinthifolia*, *Montana*, *Atlantica*, and *Myrtifolia* (Table 3). Leaves with amphistomous and partially amphistomous stomatal distributions are less common but do occur in the family and in some sections of *Schinus* (Table 3). Stomatal complex morphology, as characterized by the configuration of guard cells and subsidiary cells and their surface topography, is complex and variable within the Anacardiaceae. We recorded anomocytic and cyclocytic arrangements of the stomatal complex in the species examined, and often multiple arrangements together in a single species (Fig. 1A–C). Stomata that are level with the epidermal surface are widely present in the Anacardiaceae and characterize the more common types (Fig. 2B, D–G) of stomatal surface morphology recognized in this study. Slightly sunken stomata were observed in *Euroschinus falcata* (Fig. 2A), several species in *Schinus* sections *Montana* and *Pilifera* (Fig. 2H), and in *Lithrea caustica* (Fig. 2C) and have been previously reported in both spondioid (e.g. *Buchanania*) and anacardioid (e.g. *Rhus*, *Schinopsis*) genera (Wilkinson 1971).

All three types of simple trichomes previously reported in the Anacardiaceae (Wilkinson 1971) were observed in at least one species surveyed. Acicular trichomes (Fig. 3A) occur in all pubescent samples, conical trichomes (Fig. 3B) are present in some *Mauria* and *S. johnstonii*, forming a dense cover on both leaf surfaces in the latter (Fig. 13K), and filiform trichomes are present in *Mauria* and *Schinus* (Fig. 3A). These results confirm the ubiquity of acicular trichomes and expand the taxonomic distributions of conical trichomes (previously reported only in *Spondias* and *Semecarpus*; Wilkinson 1971) and filiform trichomes (previously reported only in *Cotinus*; Wilkinson 1971). Glandular trichomes of the species investigated herein have emergent, unicellular, or rarely bicellular bases and ovoid, globose, or cylindrical glands composed of one to several tiers of cells with each tier composed of one to several cells (Fig. 3C–F). The range of gland morphologies observed in this group is consistent with established hypotheses on the phylogenetic distribution of stalked glands within Anacardiaceae (Terrazas 1994), and their potential significance for generic or species-level systematics is discussed below.

Key differences between and within genera

Morphological comparison and multivariate statistical analysis point to several cuticular characters helpful in distinguishing between the four studied genera, but their signal is less clear among species groups in *Schinus* (Fig. 20A–D; Table 3). Similar to previous studies of cuticular characters in the Anacardiaceae (Wilkinson 1971, Terrazas 1994, Aguilar-Ortigoza *et al.* 2004), we find that trichome types may characterize higher taxa (e.g. genera, intrafamilial clades), while stomatal and epidermal cell features may distinguish species or species groups.

Of the species surveyed, acuminate-cylindrical glands are nearly ubiquitous in *Euroschinus* (Fig. 5D–F), occurring in all observed species except for *E. elegans*, and not present in any other genus, suggesting that this character may constitute a synapomorphy for the genus. Within *Euroschinus*, *E. falcata* and *E. papuana* each exhibit conspicuous cuticular features which readily distinguish them from the five New Caledonian species examined here. *Euroschinus falcata* produces abaxial axillary hairy tuft domatia (Fig. 5B) while *E. papuana* produces acuminate-cylindrical glandular trichomes with uniquely swollen, multiseriate glands (Fig. 5E).

Tuft domatia are also present in *Mauria heterophylla*, *M. subserrata*, and *M. thaumatophylla*, have been reported in *Lithrea* (but not observed in this study) and in *Rhodosphaera rhodanthema*, the sister taxon to the genera of this study, but are entirely absent in *Schinus* (Pell *et al.*, 2011; Table 3). Many species of *Mauria* produce a distinctive cylindrical glandular trichome type in which the length of the stalk is greater than or equal to the length of the gland (Fig. 8H; Gl_T3 in Fig. 20C); these glandular trichomes also tend to be clustered around well-developed areoles produced by minor order veins (Fig. 8H). The cuticular surface of *Mauria* species is further differentiated from other genera in this study by the lack of ornamentation produced on the periclinal walls of epidermal cells. Within *Mauria*, stomatal complex morphology is characterized by the presence of a peristomatal rim (Fig. 7B–D), and species can be divided into two groups based on whether outer stomatal ledges are level with (*M. cuatrecasasii*, *M. denticulata*, *M. ferruginea*, *M. sericea*, and *M. subserrata*; Fig. 7B, C) or below (*M. heterophylla*, *M. peruviana*, *M. simplicifolia*, *M. thaumatophylla*; Fig. 7D, E) this structure.

Schinus and *Lithrea* are not clearly resolved in the NMDS plot (Fig. 20A), and the two genera produce similar trichomes and stomata (Table 3). However, cuticles of each genus are readily distinguished by differences in the distinctiveness of epidermal cell periclinal walls, particularly those of guard cells, under SEM (Fig. 6, 9–19; Wilkinson 1971). Thickened epidermal cell periclinal walls and sunken stomata are prominent

protruding stomatal ledges and the thickened base of a simple acicular trichome. Scale bar = 50 μm. F, abaxial surface of *S. polygama* var. *polygama* showing stomatal complexes with protruding stomatal ledges encircled by a peristomatal rim. Scale bar = 30 μm. G, abaxial surface of *S. latifolia* showing stomatal complexes associated with radial bands of striae. Scale bar = 50 μm. H, abaxial surface of *S. latifolia* showing cyclocytic subsidiary cells, epidermal cells with undulate anticlinal walls, and the base of a simple trichome. Scale bar = 100 μm. I, abaxial surface of *S. velutina* showing cyclocytic stomatal complexes, unspecialized epidermal cells with undulate anticlinal walls, and acicular trichomes surrounded by epidermal cells with straight, thickened, anticlinal walls. J, abaxial surface of *S. polygama* showing a gland. Scale bar = 50 μm. K, adaxial surface of *S. velutina* showing undulate epidermal cells and simple trichomes. Scale bar = 100 μm. L, adaxial surface of *S. latifolia* showing epidermal cells with undulate anticlinal walls and periclinal walls ornamented with dense bands of cuticular striae. Scale bar = 50 μm.

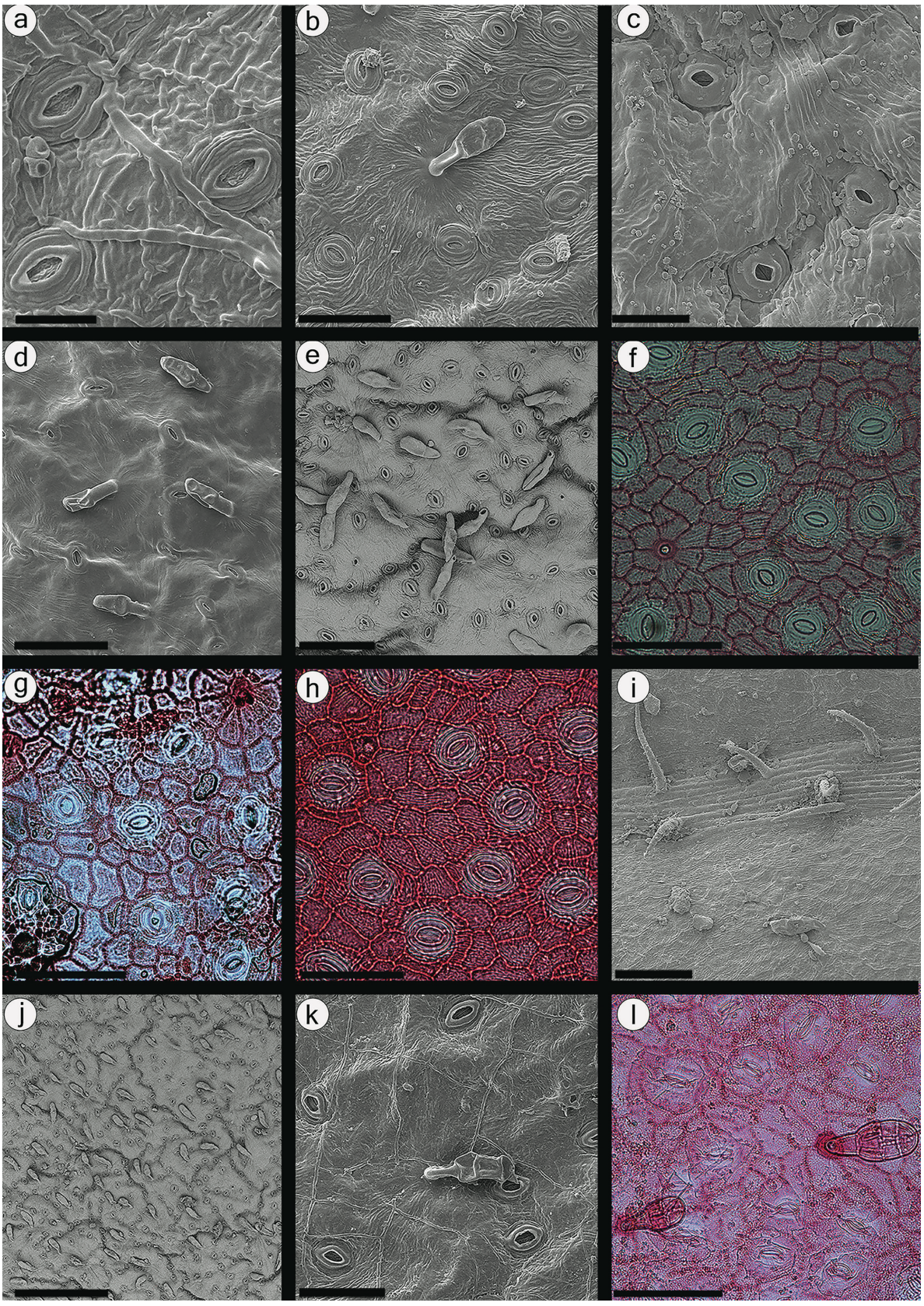

Figure 18. Stomatal and trichome characters in *Schinus* section *Myrtifolia*. A, abaxial surface of *S. venturii* showing stomatal complexes with protruding stomatal ledges, a striate peristomatal ring, and striate interior antechamber. Scale bar = 20 μm. B, abaxial surface of *S. meyeri* showing stomatal complexes, cuticular striae, and an ovoid gland. Scale bar = 50 μm. C, abaxial surface of *S. microphylla* showing stomatal complexes with prominent stomatal ledges. Scale bar = 30 μm. D, abaxial surface of *S. microphylla* showing glands, stomatal complexes, and cuticular ridges. Scale bar = 100 μm. E, abaxial surface of *S. congestiflora* showing cuticular striae, clustered ovoid glands, and stomata

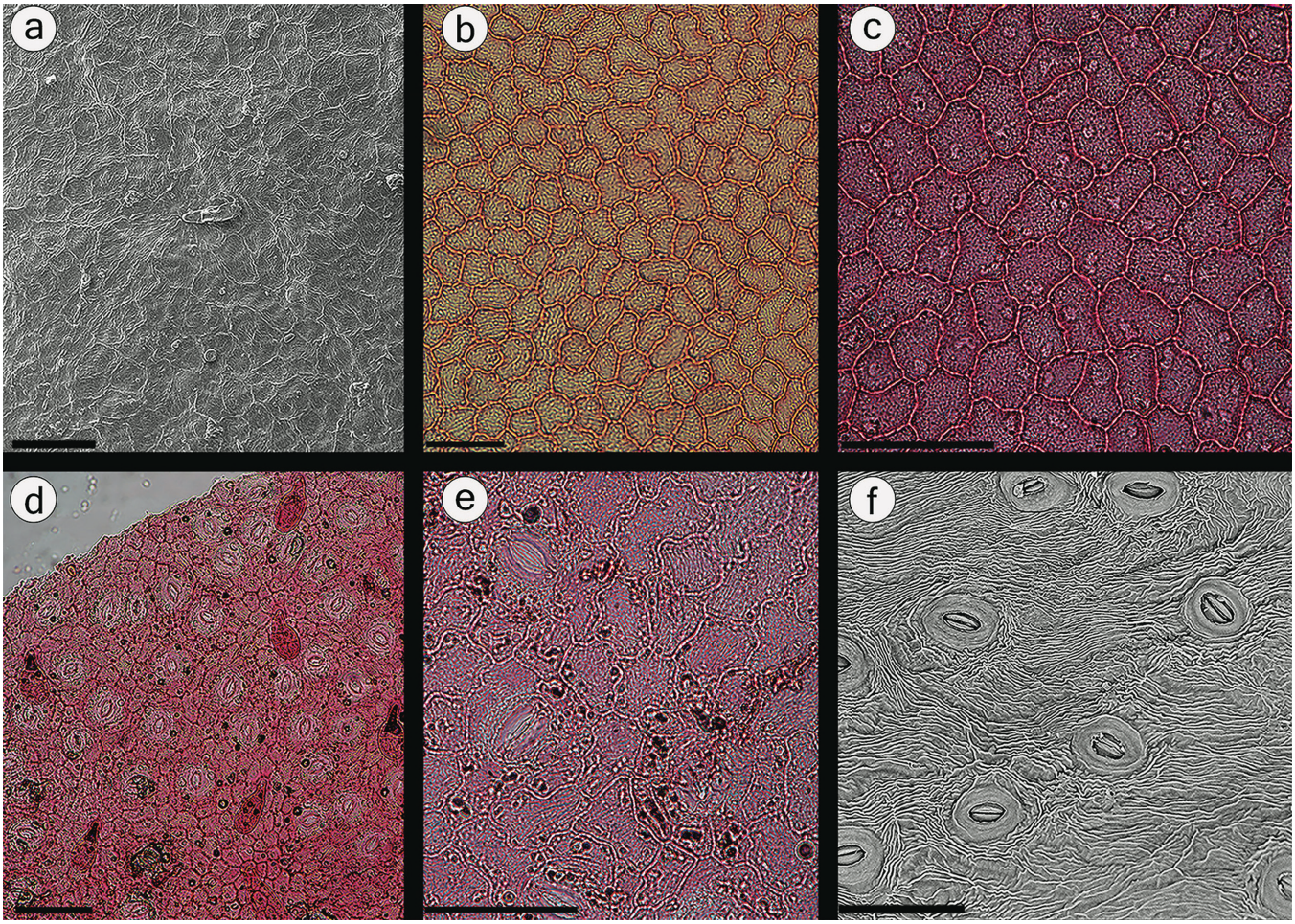

Figure 19. Epidermal cell shape and cuticular ornamentation in *Schinus* section *Myrtifolia*. A, adaxial surface of *S. venturii* showing cuticular thickenings over straight anticlinal walls and a striate surface. Scale bar = 100 μm. B, adaxial surface of *S. minutiflora* showing curved and undulate (type 3) anticlinal walls. Scale bar = 100 μm. C, adaxial surface of *S. myrtifolia* showing curved and undulate (type 3) anticlinal walls. Scale bar = 100 μm. D, abaxial surface of *S. microphylla* showing glands, stomatal complexes, and epidermal cells with straight or curved anticlinal walls. Scale bar = 100 μm. E, abaxial surface of *S. myrtifolia* showing epidermal cells with undulate (types 3, 5) anticlinal walls. Scale bar = 100 μm. F, abaxial surface of *S. myrtifolia* showing dense bands of cuticular striae. Scale bar = 50 μm.

features of *L. caustica*, which inhabits a drier ecoregion (Chilean Matorral) relative to *L. molleoides* and *L. brasiliensis*. Sunken stomata are common in Mediterranean-type climates and have also been documented in Algerian populations of *Pistacia atlantica* (Rotondi *et al.*, 2003; Belhadj *et al.*, 2007). *Schinus* is the most diverse Western Hemisphere Anacardiaceae genus in terms of number of species and exhibits much greater variability in the morphology and distribution of stomata than other genera (Fig. 20A, C; Table 3). It is the only genus reviewed for this study to include amphistomous or partially amphistomous species, species with stomatal complexes characterized by flat stomatal ledges and lacking a peristomatal rim, and species with ridged cuticle. Cuticular traits do not clearly define species groups (Fig. 20D; Table 3), but some traits co-occur in species across sections. For example, the eight *Schinus* species with stomatal complexes characterized by flat stomatal ledges and lacking a peristomatal rim (Fig. 3G, H) occur in five different sections, and seven of the eight produce adaxial stomata (Tables 3 and 4).

Stomatal distribution in *Schinus*

While evaluating the distribution of adaxial stomata for this study, discrepancies were noticed among specimens of a single

distributed in the valleys of cuticular microtopography. Scale bar = 100 μm. F, abaxial surface of *S. minutiflora* showing cyclocytic stomatal complexes. Scale bar = 100 μm. G, abaxial surface of *S. congestiflora* showing cyclocytic stomatal complexes and a trichome base surrounded by wedge-shaped epidermal cells. Scale bar = 100 μm. H, abaxial surface of *S. myrtifolia* showing cyclocytic stomatal complexes and epidermal cells with curved or undulate anticlinal walls. Scale bar = 100 μm. I, adaxial midrib of *S. minutiflora* showing simple, acicular trichomes and cuticular striae. Scale bar = 100 μm. J, abaxial surface of *S. congestiflora* showing densely distributed glands and cuticular ridges. Scale bar = 300 μm. K, abaxial surface of *S. myrtifolia* showing a gland with a unicellular stalk and cylindrical, three-tiered, multiseriate body. Scale bar = 50 μm. L, abaxial surface of *S. gracilipes* showing ovoid glands and gland bases; gland bodies have two or three tiers and are multiseriate. Scale bar = 100 μm.

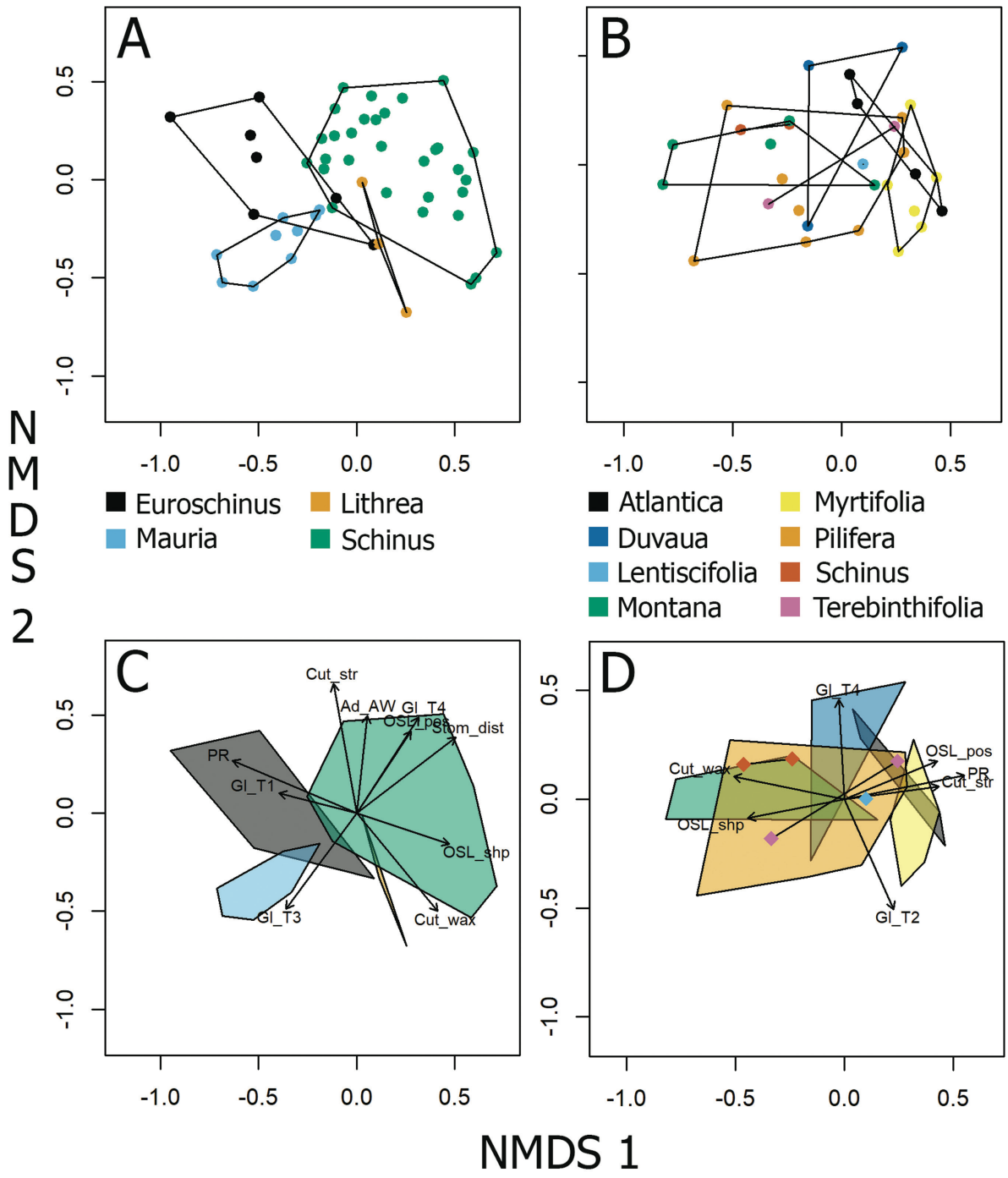

Figure 20. 2D nonmetric multidimensional scaling ordination plot showing relative disposition of species based on a matrix of 18 cuticular characters (Supporting Information, Appendix S1). A, cuticular morphospace of the four studied genera: *Euroschinus* (black dots), *Lithrea* (orange dots), *Mauria* (blue dots), and *Schinus* (green dots). Points represent species and are colour-coded by genus, and polygons are drawn around all species of each genus to delimit the total cuticular morphospace occupied by that genus. The four genera form two overlapping pairs: *Lithrea* and *Schinus* occupying relatively more positive values on axis 1 and *Mauria* and *Euroschinus* occupying relatively more negative values. B, cuticular morphospace of *Schinus* and its eight sections: *Atlantica* (black), *Duvaua* (dark blue), *Lentiscifolia* (light blue), *Montana* (green), *Myrtifolia* (yellow), *Pilifera* (orange), *Schinus* (red), and *Terebinthifolia* (magenta). Points are colour-coded by section and polygons are drawn around all species of each section to delimit the total cuticular morphospace occupied by that section. *Schinus* species sections do not occupy distinct regions of cuticular morphospace. C and D, plots A and B refigured with polygons shaded by genus (C) or section (D) and with character vectors of characters with significant correlation ($P < .001$) to cuticle samples of a particular genus or section plotted. The vector direction indicates the region of the plot of strongest correlation to the character and the vector magnitude is scaled to r^2 coefficients. Character definitions are included in Appendix S1.

Table 3. Summary of cuticular characters in *Euroschinus*, *Lithrea*, *Mauria*, and *Schinus*.

Genus or species group	Stomatal distribution	Stomatal surface morphology	Stomatal complex configuration	Gland type(s)	Tuft domatia	Epidermal cell walls	Ornamentation
Euroschinus	Hypostomous	**Type I**, II, IV	Anomocytic, cyclocytic	**Acuminate-cylindrical**	Present (*E. falcatus*)	Straight, rounded, undulate	Wax flakes, striae
Lithrea	Hypostomous	**Type III**, V	Cyclocytic, anomocytic	Short-stalked, cylindrical	?Absent[a]	Straight, rounded	Wax flakes
Mauria	Hypostomous	Type II, V	Cyclocytic, anomocytic	**Long-stalked, cylindrical**; short-stalked, ovoid	Present	Straight, rounded	N/A
Schinus sect. *Terebinthifolia*	Hypostomous, amphistomous	Type V**, VI**	Cyclocytic	Short-stalked, cylindrical	Absent	Straight, rounded	Striae
Schinus sect. *Molle*	Amphistomous	Type IV, V	Anomocytic, cyclocytic	Short-stalked, cylindrical	Absent	Straight, rounded	**Ridges**, wax flakes
Schinus sect. *Lentiscifolia*	Amphistomous	**Type VI**	Cyclocytic	Short-stalked, ovoid	Absent	Straight	N/A
Schinus sect. *Atlantica*	Hypostomous, partially amphistomous	Type V	Anomocytic, cyclocytic, staurocytic	Short-stalked, ovoid	Absent	Rounded, undulate	Striae
Schinus sect. *Pilifera*	Amphistomous, partially amphistomous	Type V, **VI, VII**	Anomocytic, cyclocytic	Short-stalked, ovoid; short-stalked, cylindrical	Absent	Straight, rounded, undulate	Wax flakes, striae, **ridges**
Schinus sect. *Montana*	Hypostomous, amphistomous	Type IV, **VII**	Anomocytic, cyclocytic	Short-stalked, cylindrical	Absent	Straight, rounded, undulate	Wax flakes, striae, **ridges**
Schinus sect. *Duvaua*	Amphistomous, partially amphistomous	Type V, **VI**	Cyclocytic	Short-stalked, ovoid	Absent	Rounded, undulate	Striae
Schinus sect. *Myrtifolia*	Hypsotomous, amphistomous	Type V	Cyclocytic	Short-stalked, ovoid	Absent	Straight, rounded, undulate	Striae, **ridges**

Bold text is used for characters which occur in only one genus. Numbered types of stomatal surface morphology are defined in the caption of Figure 2 and in Table 2.
[a]Not observed in this study but reported elsewhere (see Pell *et al.* 2011).

species and between species' evaluations in Silva-Luz *et al.* (2019; Table 4). For example, leaves of *S. fasciculata* with and without adaxial stomata were observed in this study; stomata were observed on the adaxial surface of *S. spinosa* in this study (Fig. 12A) but not by Silva-Luz *et al.* (2019); the condition in which adaxial stomata are found only along the midrib, suggested by Silva-Luz *et al.* (2019) as a character unique to *Schinus* sect. *Pilifera*, was observed in species outside this section (e.g. *S. spinosa* Fig. 12A; *S. velutina* Fig. 17A); and several species within section *Pilifera* were observed to have a scattered distribution of stomata on both surfaces (e.g. *S. bumelioides*, *S. engleri* var. *uruguayensis*). These new observations call attention to a sequence of observations that provide tentative evidence for facultative production of adaxial stomata in several species of *Schinus*. Abaxial stomatal density has been shown to vary on short evolutionary timescales in other Anacardiaceae genera (e.g. *Toxicodendron*; Ng *et al.* 2023) and adaxial stomatal distribution has been shown to vary in other species occurring in the temperate deserts of Argentina (*Prosopis flexuosa*; Giordano *et al.*, 2011). These observations raise the question of whether the observed variability of stomatal distribution in *Schinus* reflects homoplasy or phenotypic plasticity. Within *Schinus*, amphistomous species occur in each section and twice as many species are amphistomous or partially amphistomous than are hypostomous; however, only sections *Schinus*, *Pilifera*, and *Duvaua* exclusively comprise species producing adaxial stomata. This demonstrates that both field observations and controlled experiments are required to adequately characterize variability in the distribution and density of stomata in *Schinus*. Such studies are an important line of inquiry in light of the apparent deviation from the general trend of bimodal stomatal distributions among angiosperms (Muir 2015, Muir *et al.* 2023). Furthermore, studies of other ecologically diverse Anacardiaceae genera (e.g. *Pistacia*, *Rhus*) may reveal that this condition is common in the family. Wilkinson (1971, p. 442), after surveying 200 species from 46 genera, expressed the following view: 'Stomata very variable in size and density, frequently present on the adaxial surface in a few rows adjacent to or on the sides of the midrib, rarely distributed with equal frequency on both surfaces.'

Table 4. Review of assessments of stomatal distribution in *Schinus* from Wilkinson (1971), Silva-Luz *et al.* (2019), and this study.

Species	Wilkinson (1971)	Silva-Luz *et al.* (2019)	This study
S. terebinthifolia	Partially amphistomous	Hypostomous	Hypostomous
S. weinmannifolia	Amphistomous ($SD_{ab} > SD_{ad}$)	Amphistomous	Amphistomous
S. areira	N/A	Amphistomous	Amphistomous
S. molle	Amphistomous ($SD_{ab} > SD_{ad}$)	N/A	Amphistomous
S. lentiscifolia	N/A	Amphistomous	Amphistomous
S. engleri	N/A	N/A	Hypostomous
S. ferox	N/A	Amphistomous	Hypostomous
S. longifolia	Partially amphistomous	N/A	Partially amphistomous
S. ramboi	N/A	Amphistomous	Partially amphistomous
S. spinosa	N/A	Hypostomous	Partially amphistomous
S. bumelioides	Amphistomous ($SD_{ab} = SD_{ad}$)	N/A	Amphistomous
S. engleri var. uruguayensis	Amphistomous ($SD_{ab} > SD_{ad}$)	Amphistomous	Amphistomous
S. fasciculata	N/A	N/A	Partially amphistomous
S. johnstonii	Amphistomous ($SD_{ab} > SD_{ad}$)	N/A	Amphistomous
S. pearcei	N/A	Amphistomous	Amphistomous
S. pilifera var. boliviensis	Partially amphistomous	Amphistomous	Partially amphistomous
S. sinuata	N/A	N/A	Amphistomous
S. marchandii	N/A	N/A	Amphistomous
S. montana	N/A	Hypostomous	Hypostomous
S. odonellii	Amphistomous ($SD_{ab} = SD_{ad}$)	Amphistomous	Amphistomous
S. roigii	N/A	N/A	Amphistomous
S. patagonica	N/A	Hypostomous	Hypostomous
S. latifolia	Partially amphistomus	Hypostomous	Partially amphistomous
S. polygama	Amphistomous ($SD_{ab} = SD_{ad}$)	Hypsotomous	Amphistomous
S. velutina	N/A	Hypostomous	Hypostomous
S. congestiflora	N/A	N/A	Hypostomous
S. gracilipes	N/A	N/A	Hypostomous
S. meyeri	N/A	N/A	Hypostomous
S. microphylla	N/A	Amphistomous	Amphistomous
S. minutiflora	N/A	N/A	Hypostomous
S. myrtifolia	N/A	Aypostomous	Hypostomous
S. venturii	N/A	N/A	Hypostomous

SD_{ab} refers to abaxial stomatal density and SD_{ad} refers to adaxial stomatal density. N/A, not applicable.

CONCLUSION

Cuticular traits of a monophyletic group of Anacardiaceae genera, including the South American genera *Lithrea*, *Mauria*, and *Schinus* and the Australasian genus *Euroschinus*, are described and documented using scanning electron and light micrographs. The presence of distinctive acuminate-cylindrical glands in *Euroschinus* and long-stalked cylindrical glands in *Mauria* reaffirms the systematic value of trichome characters in the Anacardiaceae, which have previously been shown to characterize groups of genera (Terrazas 1994) or species (Aguilar-Ortigoza *et al.* 2004).

Schinus includes amphistomous and hypostomous species. Among amphistomous species, the distribution of adaxial stomata is variable: adaxial stomata are scattered with equal density as those on the abaxial surface, scattered with a lower density than on the abaxial surface, or restricted to areas adjacent to the midvein and secondary vein axils on the adaxial surface. We describe the last state as partially amphistomous and note that this condition can intergrade with leaves characterized as amphistomous or hypostomous. Thus, although the term is useful for descriptive purposes, more evidence is needed to conclude that it is a stable character in a phylogenetic sense. This finding underscores the importance of consulting multiple herbarium specimens of a species when evaluating morphological characters, particularly those characters that have been shown to respond to environmental variables (e.g. light intensity, CO_2) such as stomatal density and distribution (Casson and Gray 2008, Barclay and Wing 2016, Clugston *et al.* 2017). Future studies that use herbarium specimens to investigate baseline variability in stomatal distributions of other Anacardiaceae genera or perform experiments under environmental control will elucidate the evolutionary significance of this trait.

SUPPLEMENTARY DATA

Supplementary data are available at *Botanical Journal of the Linnean Society* online.

ACKNOWLEDGEMENTS

We thank the curator of BH, K. C. Nixon, and NY researchers M. Pace and J.D. Mitchell who facilitated access to herbaria collections; J. Svitko (Cornell University) for technical assistance; D. Daly, S.K. Pell, and M.R. Carvalho for helpful comments during presentation of the research; and S.K. Pell for helpful comments on the written manuscript. This work was supported by an NSF EAR-1925552 grant to M.A.G.; T.P.M. was supported by a Cornell College of Agriculture and Life Sciences Alumni Association Undergraduate Travel Award, a Cornell College of Agriculture and Life Sciences Charitable Trust Undergraduate Research Award, and the NSF grant to M.A.G.

CONFLICT OF INTEREST

The authors declare no conflict of interest.

DATA AVAILABILITY

The data underlying this study are available in the article and the online supplementary material. Microscope slides and SEM stubs are reposited in the Cornell University Plant Anatomy Collection (CUPAC).

REFERENCES

Aguilar-Ortigoza C, Sosa V, Angeles G. Phylogenetic relationships of three genera in Anacardiaceae: *Bonetiella*, *Pseudosmodingium*, and *Smodingium*. *Brittonia* 2004;**56**:169–84. https://doi.org/10.1663/0007-196x(2004)056[0169:protgi]2.0.co;2

Baranova M. Historical development of the present classification of morphological types of stomates. *The Botanical Review* 1987;**53**:53–70.

Baranova M. Principles of stomatographic studies of flowering plants. *The Botanical Review* 1992;**58**:49–99. https://doi.org/10.1007/bf02858543

Barclay RS, Wing SL. Improving the *Ginkgo* CO_2 barometer: Implications for the early Cenozoic atmosphere. *Earth and Planetary Science Letters* 2016;**439**:158–71. https://doi.org/10.1016/j.epsl.2016.01.012

Barclay RS, McElwain J, Dilcher D *et al.* The Cuticle Database: Developing an interactive tool for taxonomic and paleoenvironmental study of the fossil cuticle record. *CFS Courier Foschungsinstitut Senckenberg* 2007;**258**:39–55.

Barthlott W, Neinhuis C, Cutler D *et al.* Classification and terminology of plant epicuticular waxes. *Botanical Journal of the Linnean Society* 1998;**1998**:237–60.

Belhadj S, Derridj A, Aigouy T *et al.* Comparative morphology of leaf epidermis in eight populations of Atlas Pistachio (*Pistacia atlantica* Desf., Anacardiaceae). *Microscopy Research and Technique* 2007;**70**:837–46. https://doi.org/10.1002/jemt.20483

Carpenter KJ. Stomatal architecture and evolution in basal angiosperms. *American Journal of Botany* 2005;**92**:1595–615. https://doi.org/10.3732/ajb.92.10.1595

Carpenter KJ. Specialized structures in the leaf epidermis of basal angiosperms: morphology, distribution, and homology. *American Journal of Botany* 2006;**93**:665–81. https://doi.org/10.3732/ajb.93.5.665

Casson S, Gray JE. Influence of environmental factors on stomatal development. *The New Phytologist* 2008;**178**:9–23. https://doi.org/10.1111/j.1469-8137.2007.02351.x

Clugston JAR, Jeffree CE, Ahrends A *et al.* Do environmental factors affect the taxonomic reliability of leaf cuticular micromorphological characters? A case study in Podocarpaceae. *Edinburgh Journal of Botany* 2017;**74**:299–343. https://doi.org/10.1017/s0960428617000233

Dilcher DL. Approaches to the identification of angiosperm leaf remains. *The Botanical Review* 1974;**40**:1–157. https://doi.org/10.1007/bf02860067

Giordano CV, Guevara A, Boccalandro HE *et al.* Water status, drought responses and growth of *Prosopis flexuosa* trees with different access to the water table in a warm South American desert. *Plant Ecology* 2011;**212**:1123–34. https://doi.org/10.1007/s11258-010-9892-9

Hardin JW, Phillips LL. Atlas of foliar surface features in woody plants. VII. *Rhus* Subg. *Rhus* (Anacardiaceae) of North America. *Bulletin of the Torrey Botanical Club* 1985;**112**:1–10. https://doi.org/10.2307/2996099

Hoff M. Deux espèces Nouvelles et révision nomenclaturale des *Euroschinus* (Anacardiaceae) de Nouvelle-Calédonie. *Botanica Helvetica* 1994;**104**:123–39.

Johnson HB. Plant pubescence: An ecological perspective. *The Botanical Review* 1975;**41**:233–58. https://doi.org/10.1007/bf02860838

Joyce EM, Appelhans MS, Buerki S *et al.* Phylogenomic analyses of Sapindales support new family relationships, rapid Mid-Cretaceous Hothouse diversification, and heterogeneous histories of gene duplication. *Frontiers in Plant Science* 2023;**14**:1063174. https://doi.org/10.3389/fpls.2023.1063174

Kürschner WM. The anatomical diversity of recent and fossil leaves of the durmast oak (Quercus petraea Lieblein/Q. pseudocastanea Goeppert) — implications for their use as biosensors of palaeoatmospheric CO2 levels. *Review of Palaeobotany and Palynology* 2002;**96**:1–30. https://doi.org/10.1016/S0034-6667(96)00051-6

Lacchia AP, Tölke EA, Carmello-Guerreiro SM *et al.* Foliar colleters in Anacardiaceae: first report for the family. *Botany* 2016;**94**:337–46.

Milligan JN, Flynn AG, Wagner JD *et al.* Quantifying the effect of shade on cuticle morphology and carbon isotopes of sycamores: present and past. *American Journal of Botany* 2021;**108**:2435–51. https://doi.org/10.1002/ajb2.1772

Mitchell JD, Mori SA. The cashew and its relatives (Anacardium: Anacardiaceae). *Memoirs of the New York Botanical Garden* 1987;**42**:1–76.

Mitchell JD, Pell SK, Bachelier JB *et al.* Neotropical Anacardiaceae (cashew family). *Brazilian Journal of Botany* 2022;**45**:139–80. https://doi.org/10.1007/s40415-022-00793-5

Morat P, Jaffre T, Tronchet F *et al.* Le référentiel taxonomique Florical et les caractéristiques de la flore vasculaire indigene de la Nouvelle-Caledonie. *Adansonia* 2012;**34**:179–221. https://doi.org/10.5252/a2012n2a1

Muir CD. Making pore choices: repeated regime shifts in stomatal ratio. *Proceedings of the Royal Society B* 2015;**282**:20151498. https://doi.org/10.1098/rspb.2015.1498

Muir CD, Conesa MA, Galmes J *et al.* How important are functional and developmental constraints on phenotypic evolution? An empirical test with the stomatal anatomy of flowering plants. *The American Naturalist* 2023;**201**:794–812. https://doi.org/10.1086/723780

Muller C. Plant–insect interactions on cuticular surfaces. In Riederer M, Muller C (eds.), *Biology of the Plant Cuticle*. Oxford: Blackwell Publishing Ltd, 2006, 398–422.

Ng M, McCormick A, Utz RM *et al.* Herbarium specimens reveal century-long trait shifts in poison ivy due to anthropogenic CO_2 emissions. *American Journal of Botany* 2023;**110**:e16225. https://doi.org/10.1002/ajb2.16225

Oksanen JS, Blanchet G, Kindt F, *et al. vegan: Community Ecology Package. R package version 2.6-4.* https://CRAN.R-project.org/package=vegan; 2022 (October 2023, date last accessed).

Payne WW. A glossary of plant hair terminology. *Brittonia* 1978;**30**:239–55. https://doi.org/10.2307/2806659

Pell SK. Molecular systematic of the cashew family (Anacardiaceae). Ph.D. Thesis. Louisiana State University, 2004.

Pell SK, Mitchell JD, Lobova T, *et al.* Anacardiaceae. In: Kubitzki K (ed.), *The Families and Genera of Vascular Plants*, Vol. **10**. New York: Springer, 2011, 7–50.

Pole M. Cuticle morphology of Australasian Sapindaceae. *Botanical Journal of the Linnean Society* 2010;**164**:264–92. https://doi.org/10.1111/j.1095-8339.2010.01086.x

Prasad M, Khare EG, Kannaujia AK, Alok. Cuticle bearing fossil leaves from Mio-Pliocene period in the Sub Himalayan zone and its phytogeographical and environmental implications. *Journal of Environmental Biology* 2013;**34**:863–75.

Ramirez JL, Cevallos-Ferriz SRS, Silva-Pineda A. Reconstruction of the leaves of two new species of *Pseudosmodingium* (Anacardiaceae) from Oligocene strata of Puebla, Mexico. *International Journal of Plant Sciences* 2000;**161**:509–19. https://doi.org/10.1086/314261

Raven JA. Selection pressures on stomatal evolution. *The New Phytologist* 2002;**153**:371–86. https://doi.org/10.1046/j.0028-646X.2001.00334.x

Rotondi A, Rossi F, Asunis C *et al.* Leaf xeromorphic adaptations of some plants of a coastal Mediterranean macchia ecosystem. *Journal of Mediterranean Ecology* 2003;**4**:25–35.

Royer DL. Stomatal density and stomatal index as indicators of paleoatmospheric CO_2 concentration. *Review of Palaeobotany and Palynology* 2001;**114**:1–28. https://doi.org/10.1016/s0034-6667(00)00074-9

Silva-Luz CL, Pirani JR, Mitchell JD *et al.* Phylogeny of *Schinus* L. (Anacardiaceae) with a new infrageneric classification and insights into evolution of spinescence and floral traits. *Molecular Phylogenetics and Evolution* 2019;**133**:302–51.

Silva-Luz CL, Mitchell JD, Daly DC *et al.* Hidden species of Anacardiaceae in the Andean cloud forests: a revision of *Schinus* section *Myrtifolia*. *Systematic Botany* 2022;**47**:1031–64.

Stace CA. Cuticular studies as an aid to plant taxonomy. *Bulletin of the British Natural History Museum (Botany)* 1965a;**4**:1–78.

Stace CA. The use of epidermal characters in phylogenetic considerations. *New Phytologist* 1965b;**65**:304–18. https://doi.org/10.1111/j.1469-8137.1966.tb06366.x

Terrazas, T. Wood anatomy of the Anacardiaceae: ecological and phylogenetic interpretation. Ph.D. Thesis, University of North Carolina, 1994.

Theobald WL, Krahulik JL, Rollins RC. Trichome description and classification. In: Metcalfe CR, Chalk L (eds.), *Anatomy of the Dicotyledons*, Vol. **1**. Oxford: Oxford University Press, 1979, 40–53.

Upchurch GR. Cuticle evolution in Early Cretaceous angiosperms from the Potomac Group of Virginia and Maryland. *Annals of the Missouri Botanical Garden* 1984;**71**:522–50. https://doi.org/10.2307/2399036

Uphof JCT. Plant hairs. In: Zimmermann W, Ozenda PG (eds.), *Encyclopedia of Plant Anatomy*, Vol. **5**. Berlin: Gebruder Borntrager, 1963, 1–206.

Weeks A, Zapata F, Pell SK *et al.* To move or to evolve: contrasting patterns of intercontinental connectivity and climatic niche evolution in 'Terebinthacae' (Anacardiaceae and Burseraceae). *Frontiers in Genetics* 2014;**5**:409. https://doi.org/10.3389/fgene.2014.00409

Wilkinson, H.P. Leaf anatomy of various Anacardiaceae with special reference to the epidermis (and some contribution to the taxonomy of the genus *Dracontomelon* Blume). Ph.D. Thesis, University of London, 1971.

Wilkinson HP. The plant surface (mainly leaf): Domatia. In: CR Metcalf, Chalk L (ed.). *Anatomy of the Dicotyledons*. Oxford: Clarendon Press, 1979, 97–167.

Wilkinson HP. Leaf anatomy of *Gluta* (L.) Ding Hou (Anacardiaceae). *Botanical Journal of the Linnean Society* 1983;**86**:375–403. https://doi.org/10.1111/j.1095-8339.1983.tb00978.x

Woodward FS. Numbers are sensitive to increases in CO_2 from pre-industrial levels. *Nature* 1987;**327**:617–8. https://doi.org/10.1038/327617a0

Xiao L, Wu Z, Guo L *et al.* Late Miocene leaves and endocarps of *Choerospondias* (Anacardiaceae) from Zhejiang, Eastern China: implications for paleogeography and paleoclimate. *Biology* 2022;**11**:1399. https://doi.org/10.3390/biology11101399

Yaojia Z, Haifeng Y, Yunxia L *et al.* Stomatal apparatus of Chinese Polypodiaceae and its systematic significance. *Journal of Lanzhou University* 1999;**35**:1–11.